Title
FILTRATION STUDIES WITH ULTRAFINE PARTICLES

Authors
Bhagat, Ashok Kumar
Wilke, Charles R.

Publication Date
1966-09-01

UCRL-16574

University of California

Ernest O. Lawrence Radiation Laboratory

FILTRATION STUDIES WITH ULTRAFINE PARTICLES

DISCLAIMER

UCRL-16574
Preprint

UNIVERSITY OF CALIFORNIA

Lawrence Radiation Laboratory
Berkeley, California

AEC Contract No. W-7405-eng-48

FILTRATION STUDIES WITH ULTRAFINE PARTICLES

Ashok Kumar Bhagat and Charles R. Wilke

September 1966

FILTRATION STUDIES WITH ULTRAFINE PARTICLES

Contents

FILTRATION STUDIES WITH ULTRAFINE PARTICLES

Ashok Kumar Bhagat and Charles R. Wilke

Department of Chemical Engineering and
Lawrence Radiation Laboratory
University of California
Berkeley, California

September 1966

ABSTRACT

A new continuous filter has been developed to filter very fine particles of about 1-6 micron size without cake formation. The slurry is filtered through a rotating filter membrane and solids are rejected as a thick slurry. A general theory has also been developed to predict the limiting filtration rate for such a filter. This theory considers the centrifugal force on the particles and their diffusion in a highly turbulent field ($6 \times 10^5 < Re_D < 11 \quad 10^5$). Shear stress on the membrane and the drag coefficients were also measured and compared with the available data in the literature. Limiting filtration rates up to 33×10^{-3} ml/sec cm^2 were obtained for the systems considered. Agreement of the correlation with experimental data for 1.3 micron polystyrene latex spheres and 6-14 micron styrene divinylbenzene copolymer latex spheres is within 35%.

I. INTRODUCTION

Various types of processing operations may arise in which it is desired to withdraw liquid continuously from a suspension of fine solids while retaining the solids in the system. Solids may be washed or extracted, for example, by introducing solvent into an agitated slurry in a vessel and removing solid-free solution containing the extracted substances. Another potential application is in continuous fermentation in which dense cultures can be developed by retention of cells in the system while nutrients and products are continuously introduced and removed. The objective of the present work was to construct such a device in which solids may be filtered continuously without cake formation, and to determine its operating characteristics.

The filter consists of a membrane supported on a rotating hollow cylindrical metal screen placed in the center of a vessel containing the suspension. Fluid outside the cylinder is forced through the membrane by external pressure and out of the system through the connections to the inside of the cylinder. The centrifugal force exerted on the particles by the rotation acts counter to the drag exerted on the particles by the fluid passing through the membrane. If the rotational speed is high enough at a given filtration rate, only liquid will reach the membrane surface and particles will be retained in the system.

II. DESIGN OF THE EXPERIMENTAL SYSTEM

The flow sheet of the system is shown in Fig. 1. It consists of a rotating filter, filter chamber, and a slurry tank. The filter membrane is properly supported on a cylindrical metal screen, which rotates in a stationary cylindrical filter chamber filled with slurry of fine particles. The screen is a hollow cylinder of 6 in. diam and 3 in. height. It is rotated from below by a motor of 1.5 hp. The filter chamber is a cylinder of 8 in. diam and 13 in. height. The central shaft supporting the screen is hollow and enters the filtrate chamber located at the top of the filter chamber. The slurry is kept in a slurry tank 20 in. diam and 24 in. height. A small impeller agitator is provided to stir the slurry. The slurry is pressurized by a high pressure nitrogen cylinder. The slurry is fed to the the filter chamber and filters through the rotating membrane tightly secured to the rotating screen. The filtrate fills the hollow rotor and overflows through the hollow shaft into the filtrate chamber which is a small vertical cylindrical tank of 4 in. diam and 4 in. height. Particles approaching the membrane are thrown away from the membrane by the centrifugal force. By carefully choosing the variables it is possible to establish conditions such that no particles will reach the membrane. The overflow from the filtrate chamber is metered through the rotameters. A pressure tap is located 1/8 in. away from the membrane to indicate static liquid pressure. A mechanical seal and ball bearing are provided at both ends of the filter chamber. Detailed description of the equipment is given in Chapter IV.

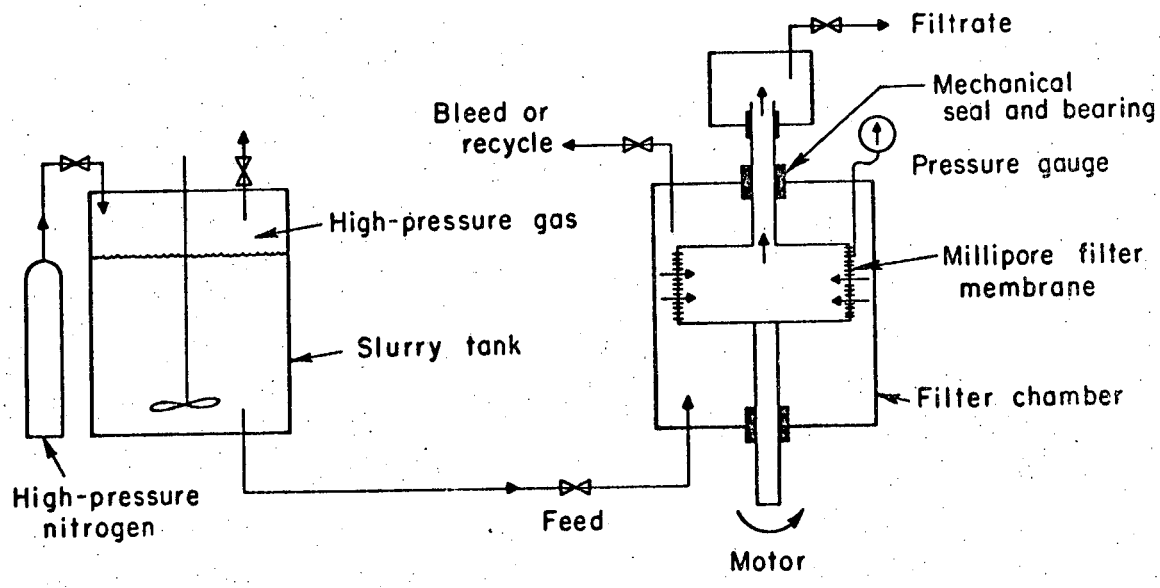

FLOW SHEET – EXPERIMENTAL SYSTEM

MUB-9709

Fig. 1. Flow sheet of the experimental system.

system. Equation (4) can be transformed to give Eq. (5).

$$\frac{dQ}{d\theta} = -kQ^m \tag{5}$$

where

Q = rate of filtration (ml/sec) = $\frac{dV}{d\theta}$

m = a constant $m = 3-n$

Equation (5) can be integrated to give Eq. (6) with the condition that

$$Q = Q_0 \text{ at } \theta = 0 \quad \frac{1}{(m-1)}\left[\frac{1}{Q^{(m-1)}} - \frac{1}{Q_0^{(m-1)}}\right] = k\theta \tag{6}$$

where

Q_0 is the initial filtration rate.

If the resistance to filtration R is defined as (see Section B)

$$R = \frac{\Delta P}{Q/A} \tag{7}$$

Eq. (6) can be written as

$$R^{(m-1)} = R_0^{(m-1)} + k'\theta \tag{8}$$

where R_0 is the initial resistance to filtration and k' is given by Eq. (9)

$$k(m-1)(\Delta P\, A)^{(m-1)} = k' \tag{9}$$

There are four basic laws of filtration proposed by Hermans and Bredeé.

1. Cake Law. The following equation was derived for cake filtration assuming the flow of liquid through a group of parallel

cylindrical capillary tubes of constant diameter and increasing length and such flow obeying Poiseuille's law for capillary flow.

$$\frac{\theta}{V} = \frac{k}{2} V + \frac{1}{Q_0} \qquad (10)$$

Equation (10) is the case for n=0 in Eq. (4) and is same as the integrated form of Eq. (3).

2. Law of Complete Blocking. If the filtering medium is regarded as a collection of parallel capillary tubes of constant diameter and length and which become blocked in such a way that every time a particle passes into a capillary it is completely sealed, then Eqs. (11) and (12) can be easily derived.

$$Q_0 - Q = kV \qquad (11)$$

$$V = \frac{Q_0}{k} (1 - e^{-k\theta}) \qquad (12)$$

Equations (11) and (12) can be combined to give Eq. (13). This is the case for n = 2 in Eq. (4).

$$Q = Q_0 e^{-k\theta} \qquad (13)$$

3. Standard Law. If the filter is considered to consist of a set of parallel capillary tubes of constant length and their diameter decreases gradually and regularly by the adsorption of precipitate against the walls of the tubes in such a way that the inside volume of the tubes decreases proportionally to the volume of the filtrate passed through, the Eq. (14) can be derived. This corresponds to n = 3/2 in Eq. (4).

$$\frac{\theta}{V} = \frac{k}{2} \theta + \frac{1}{Q_0} \qquad (14)$$

According to Hermans and Bredee most of the filtrations which do not obey the cake law obey the standard law. Daniels and Hale[5] found that filtration of tissue culture media obeyed the standard law.

4. Intermediate Law. This follows the characteristics of both the cake law and standard law. Although the exact mode of plugging is not known the following equation was obtained empirically.

$$\frac{1}{Q} - \frac{1}{Q_0} = k\theta \qquad (15)$$

here $n = 1$

Grace[10] in an excellent work on the structure and performance of filter media, correlated the pore structure of filtering media with their plugging rates. These plugging rates were obtained from the standard law by plotting the data collected during clarification of dilute carbonyl iron suspension. Grace found that such filtrations could be divided into 3 periods. The initial period conformed to no filtration theory. Then an extended period of filtration follows the standard law. When 50 to 80 percent of the filtrate volume theoretically required to cause complete plugging had passed it enters the cake law period after going through a transition zone. The retention mechanism in filtration is very nicely illustrated in Hand Book of Filtration.[8]

B. Resistance Concept in Filtration

The resistance R to flow through a cake and the membrane can be defined as

$$R = \frac{\Delta P}{q} \qquad (16)$$

where

ΔP = effective pressure drop across the cake and the membrane (g_f/cm^2)

q = filtration rate/area (ml/sec cm^2)

The total resistance of a membrane and a cake of thickness L can be given by Eq. (18)

$$R = R_0 + \beta L \tag{17}$$

where

β = thickness coefficient of cake resistance or cake resistance/thickness (g_f sec/ml cm)

R_0 = resistance of clean membrane (g_f sec/ml)

However if w is the weight of dry cake/area, R can also be expressed as

$$R = R_0 + \beta' w \tag{18}$$

where

β' = cake resistance/(weight of cake/area) (g_f sec/g cm)

It will be noted that β is quite analogous to specific resistivity of electrical conduction. The general equation of constant pressure filtration with cake deposition is given by Eq. (3). It can be rearranged to give

$$R = \frac{\Delta P}{q} = \frac{\mu \alpha w}{A g_c} + \frac{\mu}{g_c} R_m \tag{19}$$

if ρ_c is the density of the dry cake

$$W = \rho_c A L \tag{20}$$

Substituting for W in Eq. (19) and comparing with Eq. (17) we get

$$R_0 = \frac{\mu}{g_c} R_m \tag{21}$$

$$\beta = \frac{\mu}{g_c} \alpha \rho_c \tag{22}$$

from Eqs. (17) and (18) it can be shown

$$\beta'(1-\epsilon) = \beta \rho_p \tag{23}$$

where ρ_p = density of particles (g/cm^3)
ϵ = porosity of cake.

C. Centrifugal System

1. Development of the Equation for Limiting Filtration Rate

The rotation of the filter membrane in the filter chamber develops a tangential velocity distribution in the annulus. The tangential velocity of the liquid layer adjacent to the filter membrane is the same as that of the membrane, and that of the liquid layer adjacent to the filter chamber wall is zero. A great portion of the velocity change occurs within a short distance away from the two surfaces. A qualitative plot of the tangential velocity distribution in the annulus is given in Fig. 2. Above a certain rpm turbulence develops in the annulus.

a. Tangential Velocity Distribution in the Annulus. The laminar flow of an incompressible fluid between two coaxial vertical cylinders has been discussed by Schlicting[16] and the necessary equations for velocity profile and shear stress developed. However, no experimental or analytical work is available for turbulent flow. An approximate solution for a very short distance away from the membrane can be obtained. For small distance away from the membrane (50 microns or less) the curvature of the rotor can be neglected and the problem can be approximated by the case of liquid flowing past a flat plate. Von Karman's[19] universal

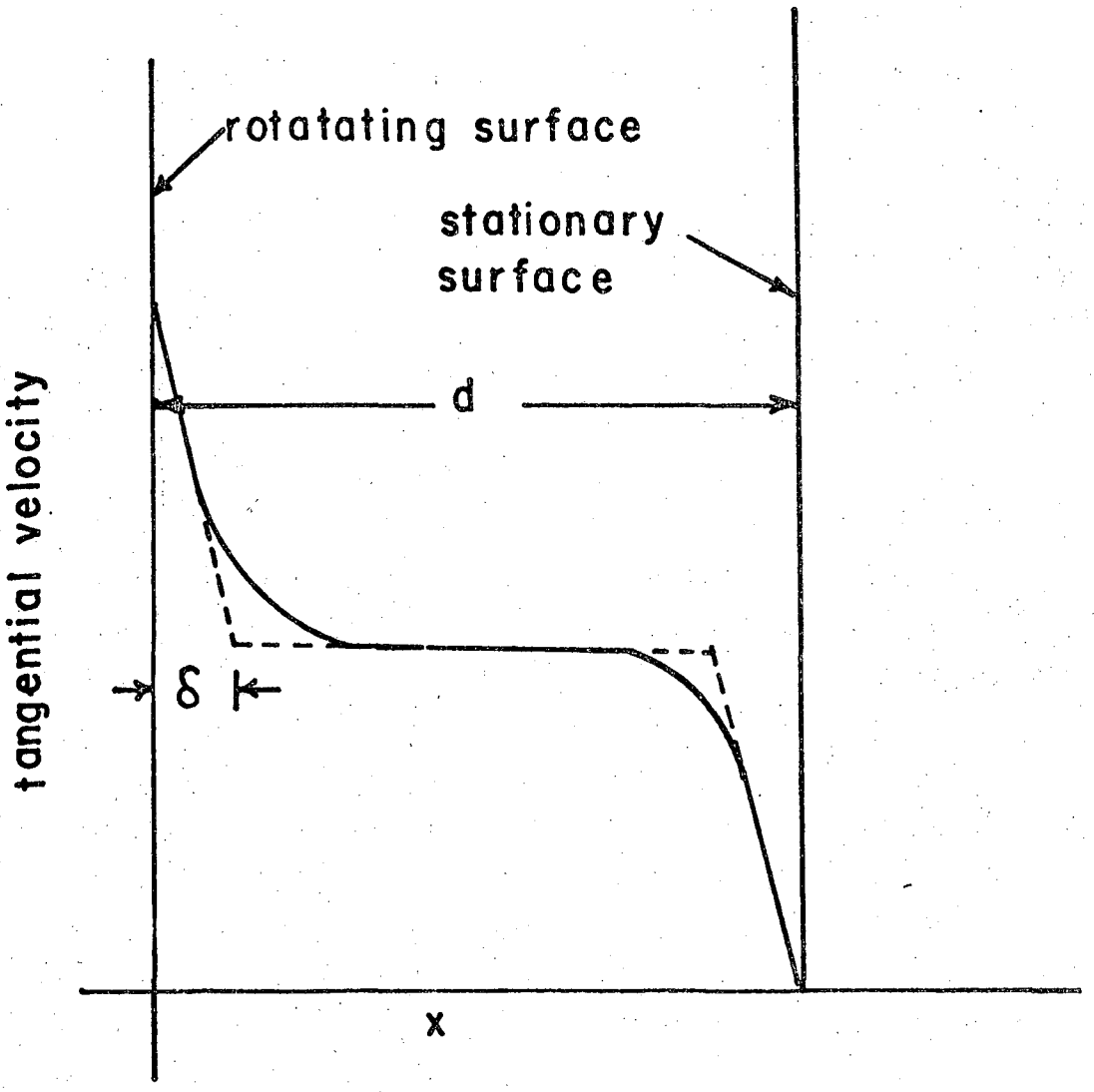

MUB-12799

Fig. 2. Tangential velocity profile in the annulus.

velocity distribution for turbulent flow can be used in the following form:

$$v^{+'} = x^{+} \qquad \text{for } x^{+} < 5 \tag{24}$$

where

$$v^{+'} = \frac{v'}{v_\tau} \tag{25}$$

$$x^{+} = \frac{v_\tau}{\nu} x \tag{26}$$

$$v_\tau = \sqrt{\frac{\tau_w g_c}{\rho}} \tag{27}$$

v' = tangential velocity of liquid relative to the membrane (cm/sec)

ν = kinematic viscosity of liquid (cm^2/sec)

τ_w = shear stress at the membrane surface (g_f/cm^2)

v_τ = shear velocity (cm/sec)

x = distance away from the membrane (cm).

$$v = v_0 - v' \tag{28}$$

where v_0 = tangential velocity of the membrane (cm/sec)

v = tangential velocity of any liquid layer (cm/sec)

Substituting for v' from Eqs. (25), (26) and (27) we get

$$\frac{v}{v_0} = (1 - ax) \tag{29}$$

where

$$a = \frac{\tau_w g_c}{\mu v_0} \tag{30}$$

Equation (29) approximately gives v at any x. In the derivation of Eq. (29) it has been assumed that there is no radial flow of liquid. In fact there is a radial flow of liquid into the membrane which could

change the velocity distribution near the membrane. No attempt has been made here to make this correction in absence of information on the effect of radial flow.

b. Simple Centrifugal Force Model. Any particle moving with a tangential velocity v in circular path of radius r experiences a centrifugal force F_c given by

$$F_c = \frac{\pi}{6} D_p^3(\rho_p-\rho) \frac{v^2}{rg_c} \tag{31}$$

where D_p = particle diam (cm)
ρ_p = density of particles (g/cm^3)
r = radius of the path (cm)
F_c = centrifugal force (g_f)

Substituting for v from Eq. (29)

$$F_c = \frac{\pi}{6} D_p^3(\rho_p-\rho)\frac{v_0^2}{rg_c} (1-ax)^2 \tag{32}$$

This centrifugal force F_c acts to throw the particle away from the membrane. The filtrate flowing radially into the membrane exerts a drag force F_d on the particle. F_d in general is given by Eq. (33).

$$F_d = C_d A_p \rho\frac{u^2}{2g_c} \tag{33}$$

where C_d = drag coefficient
F_d = drag force (g_f)
A_p = projected area of particle in the direction of motion (cm^2)
u = radial liquid velocity (cm/sec)

For small spherical particles and small radial liquid velocity such that $Re_p < 0.3$ Eq. (33) reduces to Stoke's Law.

$$C_d = 24/Re_p \quad \text{where} \quad Re_p = \frac{D_p u}{\nu}$$

Re_p = Reynold's number based on particle diam

$$F_d = \frac{1}{g_c} 3\pi\mu u D_p \tag{34}$$

where μ = viscosity of liquid (poise).

Equation (34) gives the drag force on a single particle falling in a stagnant liquid. If we assume that the rotation and turbulence do not effect the drag coefficient C_d appreciably, Eq. (34) can be used to calculate F_d in the present physical situation also.

A particle under the influence of these forces is shown in Fig. 3. All forces are in the horizontal plane and in the radial direction. Qualitative plots of v and centrifugal pressure P_c (to be discussed in Sec. C.3) are given in the vicinity of the membrane. In order that the particle does not reach the membrane we must have

$$F_c \geq F_d \tag{35}$$

or

$$\frac{\pi}{6} D_p^3(\rho_p-\rho)\frac{v_0^2}{rg_c}(1-ax)^2 \geq \frac{1}{g_c} 3\pi\mu u D_p$$

or

$$u \leq \frac{D_p^2(\rho_p-\rho)}{18\mu} \frac{v_0^2}{r}(1-ax)^2$$

at the membrane surface $x = 0$ and $r = D_i/2$

where D_i = diameter of the inner rotor.

If $Z_0 = \frac{2v_0^2}{D_i g}$ (centrifugal effect factor)

$$u \leq \frac{D_p^2(\rho_p-\rho)g}{18\mu} Z_0 \tag{36}$$

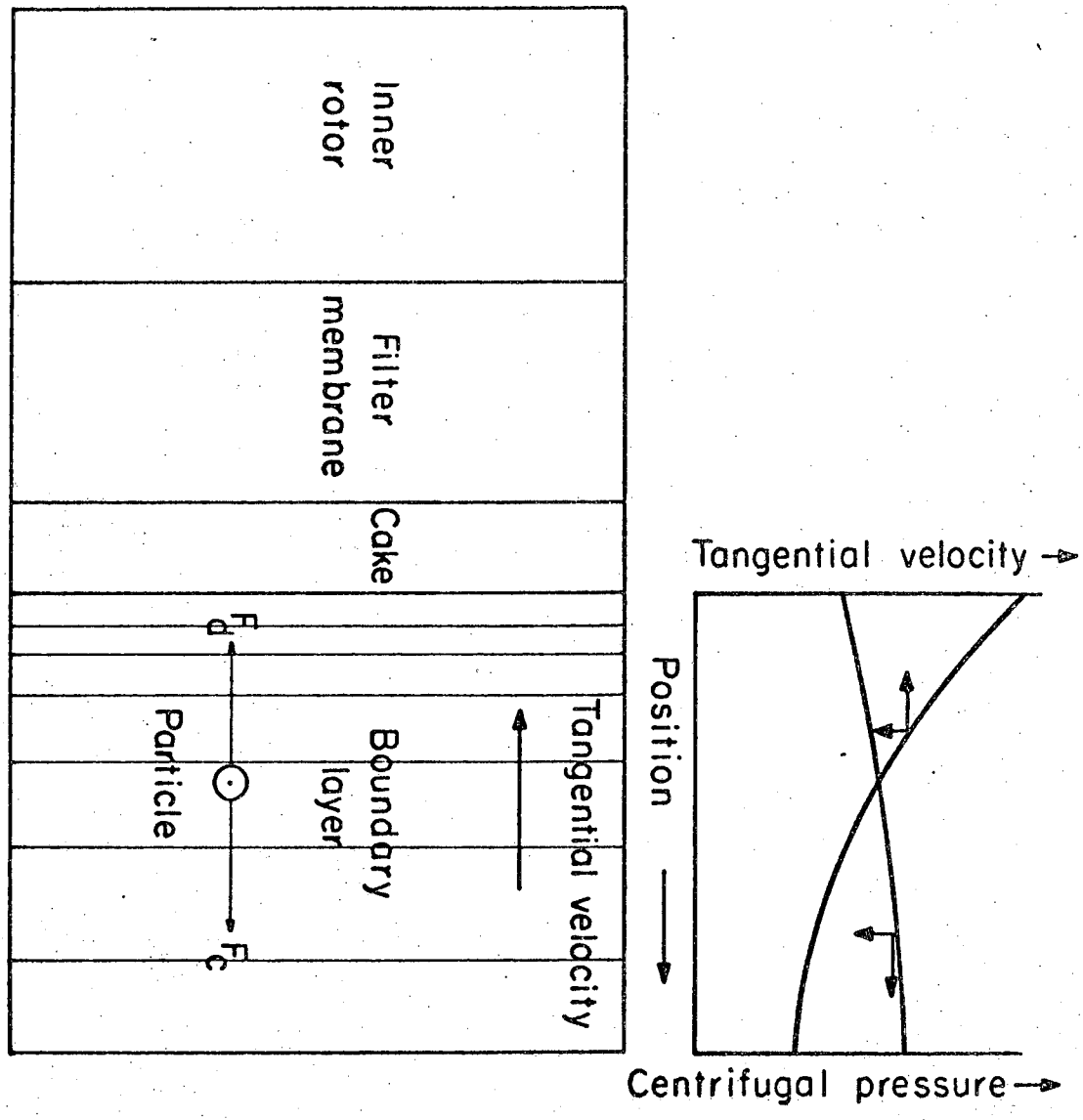

Fig. 3. A particle under the influence of centrifugal and drag forces in the annulus.

Equation (36) establishes a condition for no cake formation. In this case

$$u = q = \frac{1}{A} \frac{dV}{d\theta} \tag{37}$$

For a given set of operating conditions Eq. (36) sets the limit on the maximum filtration rate/area which can be obtained without cake formation. If we start a filtration run with a ΔP such that a high q is obtained. Particles will reach the membrane and the cake resistance will increase and q will decrease with time. After some time q will reach such a value that no more particles will reach the membrane. Filtration can be continued in principle at this constant q for any length of time. This constant filtration rate is called the limiting filtration rate, q_∞.

c. Improved Model Including the Effect of Particle Diffusion. In the simple centrifugal force model only forces acting on a particle were considered. If the drag force is large, particles will move towards the membrane and the particle concentration near the membrane will increase and a concentration gradient is developed near the membrane surface. As the result of the concentration gradient particles tend to move away from the surface region by molecular and turbulent diffusion. Fig. 4 illustrates this model. In this physical situation there are three main fluxes: 1) convective flux 2) diffusion flux 3) centrifugal flux.

Introducing the centrifugal flux term in the diffusion equation in terms of mass fluxes as developed by Bird, Stewart, and Lightfoot,[2]

$$n_p = c(n_p+n_\ell) - \rho_s(D+\epsilon) \frac{dc}{dx} + u_t \rho_s c \tag{38}$$

where n_p = mass flux of particles with respect to fixed coordinates (g/cm^2 sec)

n_ℓ = mass flux of liquid with respect to fixed coordinates (g/cm^2 sec)

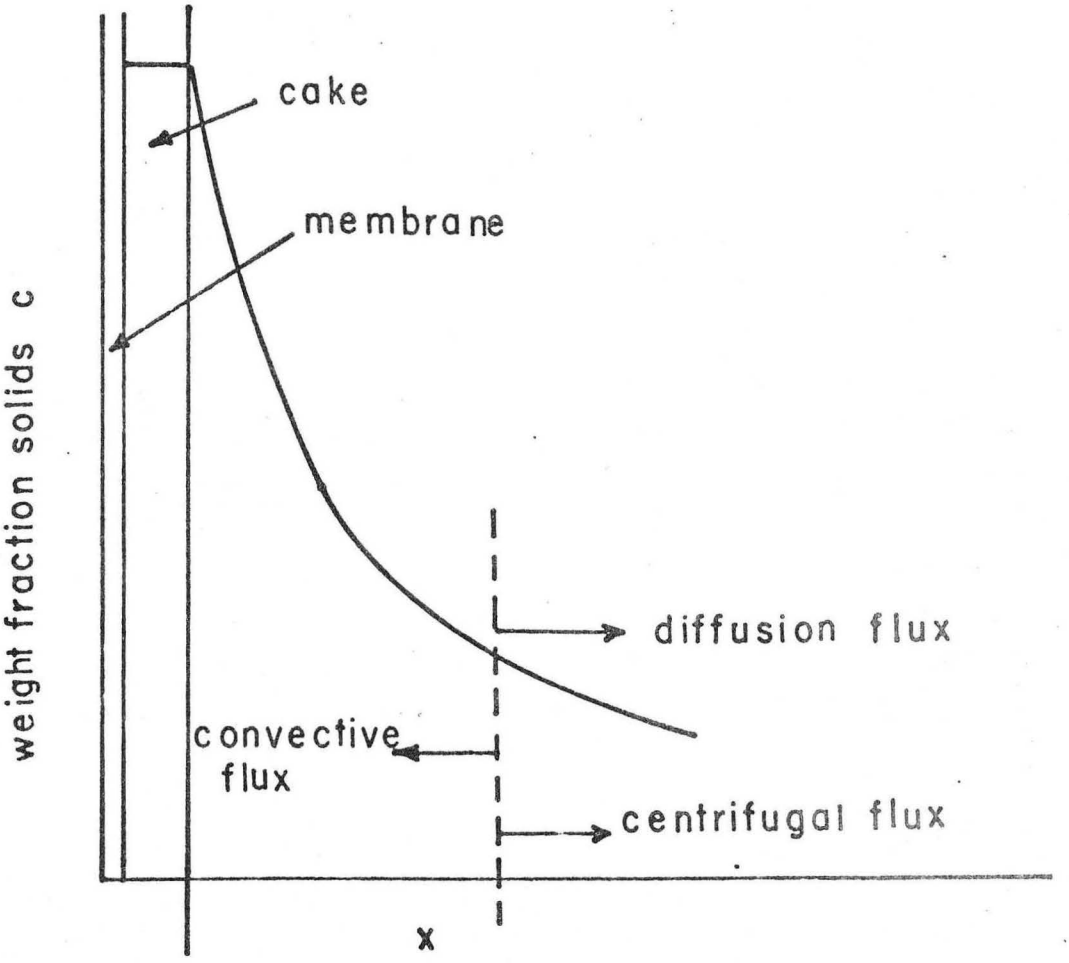

Fig. 4. Theoretical model showing the effect of particle diffusion.

ρ_s = density of slurry (g/cm^3)

u_t = terminal velocity of particles under the effect of centrifugal force (cm/sec)

c = weight fraction of solids

D = molecular diffusivity of particles (cm^2/sec)

ϵ = eddy diffusivity (cm^2/sec)

At steady state and when the limiting filtration rate has been reached (i.e., no more cake is formed) no net flux of particles occurs across any vertical plane. Thus $n_p=0$ and

$$-(D+\epsilon)\frac{dc}{dx} = c\left(-\frac{n_\ell}{\rho_s} - u_t\right) \tag{39}$$

but $n_\ell = -\rho u$

$$-(D+\epsilon)\frac{dc}{dx} = c\left(\frac{\rho}{\rho_s}u - u_t\right) \tag{40}$$

The terminal velocity u_t is the velocity of the particle relative to liquid which it aquires due to the centrifugal force. From Eq. (36) u_t is

$$u_t = \frac{D_p^2(\rho_p-\rho)g}{18\mu} Z_0(1-ax)^2 \tag{41}$$

at x=0

$$u_{t0} = \frac{D_p^2(\rho_p-\rho)g}{18\mu} Z_0 \tag{42}$$

therefore

$$u_t = u_{t0}(1-ax)^2$$

It is assumed here that at every position of x, the particle instantaneously acquires its terminal velocity.

$$-\int\frac{dc}{c} = \frac{\rho u}{\rho_s}\int\frac{dx}{(D+\epsilon)} - u_{t0}\int\frac{(1-ax)^2dx}{(D+\epsilon)} + k$$

where k is a constant of integration.

The eddy diffusity ϵ is a function of x. The functional dependence of ϵ on x in rotating cylinders has not been investigated. However for the turbulent flow in pipes a large number of empirical equations have been reported in the literature. Wasan, Tien, and Wilke[20] have recently developed an expression for eddy diffusivity which gives good results in the correlation of mass and heat transfer. According to them

$$\frac{\epsilon}{\nu} = \frac{4.16\times10^{-4}x^{+3} - 15.15\times10^{-6}x^{+4}}{1 - 4.16\times10^{-4}x^{+3} + 15.15\times10^{-6}x^{+4}} \qquad (43)$$

for $0 \leq x^{+} \leq 20$

for small values of $x^{+} < 5$ Eq. (43) can be approximated by

$$\frac{\epsilon}{\nu} = 4.16\ 10^{-6}x^{+3} \qquad (44)$$

From Eqs. (26), (27), and (44) we have

$$\epsilon = 4.16\times10^{-4}\left(\frac{\tau_w g_c}{\rho}\right)^{3/2}\ \frac{x^3}{\nu^2} \qquad (45)$$

or

$$\epsilon = \epsilon_0 x^3 \qquad (46)$$

where

$$\epsilon_0 = \frac{4.16\times10^{-4}}{\nu^2}\ \left(\frac{\tau_w g_c}{\rho}\right)^{3/2} \qquad (47)$$

To the first very crude approximation it can be assumed that the growth of turbulence in this system is identical to that for turbulent flow in pipes. Under this assumption the eddy diffusivity ϵ given by Eq. (45) can be used in Eq. (40).

To estimate the molecular diffusivity, D of large spherical particles, Wilke and Chang[21] recommend the Stokes-Einstein equation in

the following form.

$$D = \frac{kT}{3\pi\mu D_p} \tag{48}$$

where k = Boltzman constant, 1.37×10^{-16} ergs/°C

T = temperature (°K)

μ = liquid viscosity (poise)

D_p = particle diameter (cm)

With these approximate values of ϵ and D Eq. (40) can be solved.

$$-\ell n\, c = \frac{\rho\mu}{\rho_s \epsilon_0} \int \frac{dx}{(A^3+x^3)} - \frac{u_{t0}}{\epsilon_0}\left[\int \frac{dx}{(A^3+x^3)} - 2a \int \frac{x\,dx}{(A^3+x^3)}\right. \tag{49}$$

$$\left. + a^2 \int \frac{x^2 dx}{(A^3+x^3)}\right] + k$$

where $$\frac{D}{\epsilon_0} = A^3 \tag{50}$$

Substituting the proper values of the integrals[7] in Eq. (45) we get

$$-\ell n\, c = \frac{\frac{u\,\rho}{\rho_s} - u_{t0}}{\epsilon_0}\left[\frac{1}{6A^2}\,\ell n\,\frac{(A+x)^2}{(A^2 - A\,x+x^2)} + \frac{1}{A^2\sqrt{3}}\,\tan^{-1}\frac{2x-A}{A\sqrt{3}}\right]$$

$$+ \frac{2au_{t0}}{\epsilon_0}\left[\frac{1}{6A}\,\ell n\,\frac{(A^2-Ax+x^2)}{(A+x)^2} + \frac{1}{A\sqrt{3}}\tan^{-1}\frac{2x-A}{A\sqrt{3}}\right]$$

$$- \frac{u_{t0}}{3\epsilon_0}\,\ell n(A^3+x^3) + k \tag{51}$$

To obtain the constant of integration, k in Eq. (51) we have the following boundary condition

$$\text{at} \quad x = \delta \quad c = c_b \tag{52}$$

c_b is the weight fraction of the particles in the bulk of the slurry in the filter chamber. The boundary layer thickness δ is arbitrarily defined as:

$$\text{at} \quad x = \delta \quad v = 1/2 \; v_0 \tag{53}$$

From Eq. (29)

$$\delta \simeq \frac{1}{2a} \tag{54}$$

However for steady state and the case of limiting filtration rate, i.e., incipient cake formation

$$c = c_w \quad \text{at } x = 0 \tag{55}$$

where c_w = weight fraction of the particles in the bulk of the cake. The distance x is measured from the surface of the cake. From conditions (52) and (55)

$$\ell n \frac{c_w}{c_b} = \frac{\frac{\rho}{\rho_s} u - u_{t0}}{\epsilon_0} \left[\frac{1}{6A^2} \ell n \frac{(A+\delta)^2}{(A^2-A\delta+\delta^2)} + \frac{1}{A^2\sqrt{3}} \left\{ \tan^{-1} \frac{2\delta-A}{A\sqrt{3}} - \tan^{-1} \left(\frac{-1}{\sqrt{3}} \right) \right\} \right] + \frac{2a \; u_{t0}}{\epsilon_0} \left[\frac{1}{6A} \ell n \frac{(A^2-A\delta+\delta^2)}{(A+\delta)^2} + \frac{1}{A\sqrt{3}} \left\{ \tan^{-1} \frac{2\delta-A}{A\sqrt{3}} - \tan^{-1} \left(\frac{-1}{\sqrt{3}} \right) \right\} \right] - \frac{u_{t0}}{3\epsilon_0} \ell n \left(\frac{A^3+\delta^3}{A^3} \right) \tag{56}$$

If $A \ll \delta$ (which applies to the present case)

$$\ell n \frac{c_w}{c_b} = \frac{\frac{\rho}{\rho_s} u - u_{t0}}{\epsilon_0} \quad \frac{1}{A^2\sqrt{3}} \frac{2}{3}\pi + \frac{2au_{t0}}{\epsilon_0} \quad \frac{1}{A\sqrt{3}} \frac{2}{3}\pi$$

$$- \frac{u_{t0}}{3\epsilon_0} \quad \ell n\left[1+\left(\frac{\delta}{A}\right)^3\right] \tag{57}$$

In most of the cases second and third terms on the right hand side of Eq. (57) are much smaller than the first term and can be neglected.

$$\ell n \frac{c_w}{c_b} \simeq \frac{\frac{\rho}{\rho_s} u - u_{t0}}{\epsilon_0} \quad \frac{1}{A^2\sqrt{3}} \frac{2}{3}\pi \tag{58}$$

for dilute slurries $\frac{\rho}{\rho_s} \simeq 1.0$

$$u = u_{t0} + \frac{3\sqrt{3}}{2\pi} A^2 \epsilon_0 \ell n \frac{c_w}{c_b} \tag{59}$$

$$u = u_{t0} + u_d \tag{60}$$

where the diffusion term u_d is given by Eq. (61)

$$u_d = \frac{3\sqrt{3}}{2\pi} A^2 \epsilon_0 \ell n \frac{c_w}{c_b} \tag{61}$$

$$u_d = 0.0613\, v_\tau \left(\frac{D}{\nu}\right)^{2/3} \ell n \frac{c_w}{c_b} \tag{62}$$

The limiting filtration rate/area can thus be predicted by Eq. (60) where u_{t0} and u_d are estimated from Eqs. (42) and (62) respectively.

2. Fluid Mechanics of the System

The fluid mechanics of the flow of a viscous liquid between two concentric rotating cylinders has been a subject of great interest.

Measurements of the torque transmitted to the outer cylinder as a function of the angular velocity of the inner rotor and the gap width are used to determine the onset of instability in laminar flow. For the case of finite gap between the cylinders, the analysis of the stability problem is given by Chandrasekhar[4] in terms of a critical Taylor number T_c above which the flow is turbulent. Taylor number T is given by

$$T = \frac{4}{9} D_i^4 \left(\frac{\omega}{\nu}\right)^2 \tag{63}$$

For our system $D_i = 6$ in., $N = 1000$ (typically),
and $\nu = 0.9 \times 10^{-2}$ cm^2/sec
Taylor number for our system = 3.12×10^8 which is much higher than the critical Taylor number of 3.1×10^4 defined by Chandrasekhar. Donnelly and Simon[6] have analyzed the available data and have obtained an empirical relationship between the torque transmitted and the angular velocity. At speeds well beyond critical they found that the torque G varies approximately as $\omega^{1.5}$ and $d^{0.31}$ where d is the gap width. Bachelor in the same paper[6] provides a theoretical basis for these relations. He assumes a steady flow and a flow pattern in the axial plane as sketched in Fig. 5. The distribution of vorticity in the inviscid core has been given by Bachelor.[1]

3. Drag Coefficient for Rotating Cylinders

The shear stress, developed on the surface of inner rotating cylinder can be expressed in the form of a drag coefficient C_D

$$\tau_w = C_D \rho \frac{v_0^2}{2g_c} \tag{64}$$

Theodorsen and Regier[18] have reported measurements of the drag on cylinders rotating in various fluids. They have correlated their data as

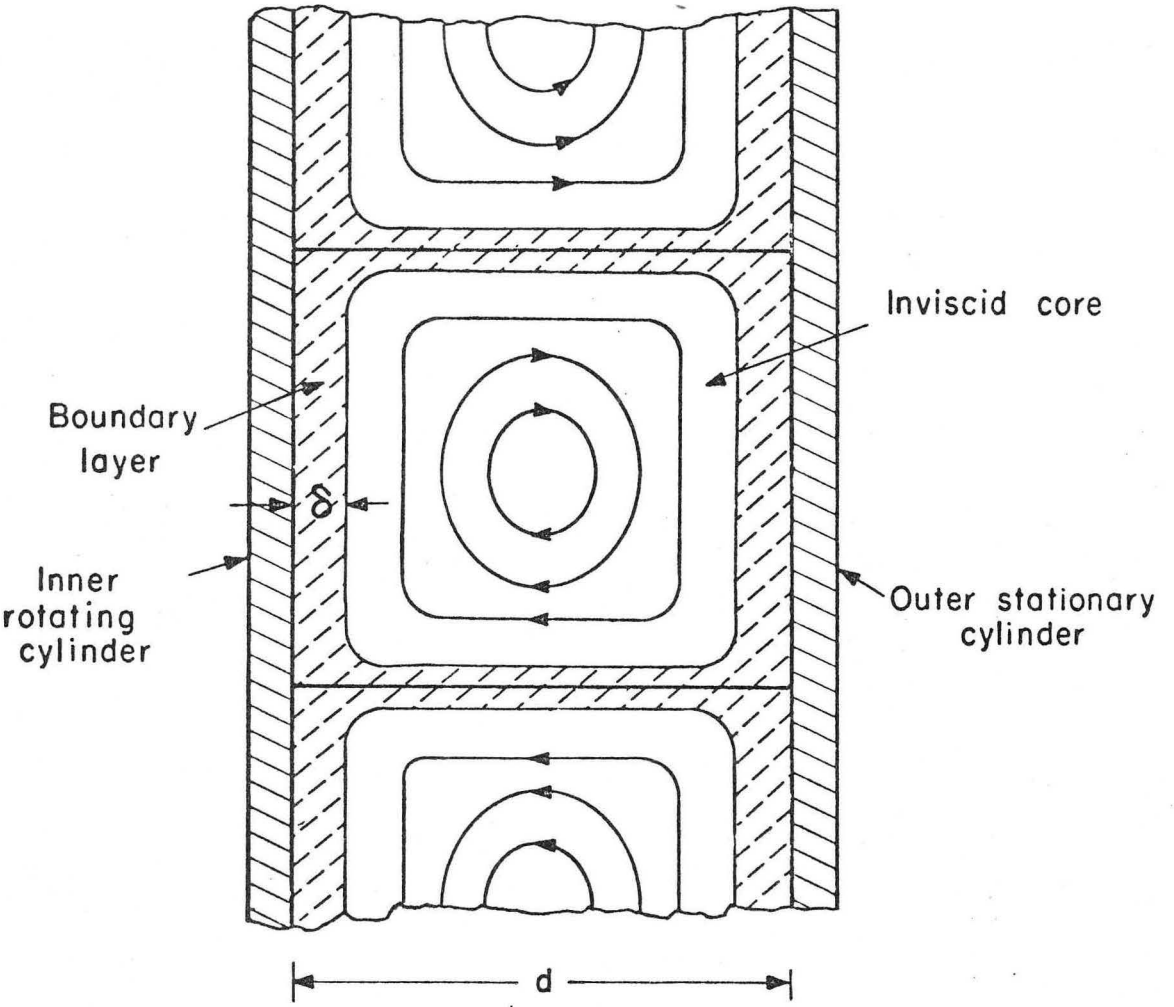

Fig. 5. Steady flow pattern in the axial plane as assumed by Bachelor.[6]

$$\frac{1}{\sqrt{C_D}} = -0.6+4.07 \log_{10} Re_D \sqrt{C_D} \qquad (65)$$

where Re_D = Reynolds number based on rotor diameter

$$Re_D = \frac{v_o D_i}{2\nu} \qquad (66)$$

Their data are reproduced in Fig. 22 and compared with our measurements of drag coefficients.

4. Centrifugal Pressure

The liquid in the rotor rotates with the same angular velocity as the rotor. This develops a centrifugal pressure P_c on the inside of the filter membrane. Consider an element of liquid in the form of a thin hollow cylinder of radius r and thickness dr and height h as shown in Fig. 6.

mass of this liquid	$= 2\pi r\, dr\, h\, \rho$
centrifugal force on this mass of liquid	$= \frac{1}{g_c} (2\pi r\, dr\, h\, \rho) r\, \omega^2$ (in g.f. units)
this force is exerted on an area	$= 2\pi r\, h$

Centrifugal pressure dP_c developed by this mass of liquid is given by

$$dP_c = \frac{(2\pi r\, dr\, h\, \rho) r\, \omega^2}{2\pi r\, h\, g_c}$$

or

$$\frac{dP_c}{dr} = \frac{\rho\, r\, \omega^2}{g_c} \qquad (67)$$

as ω is constant for all r we get

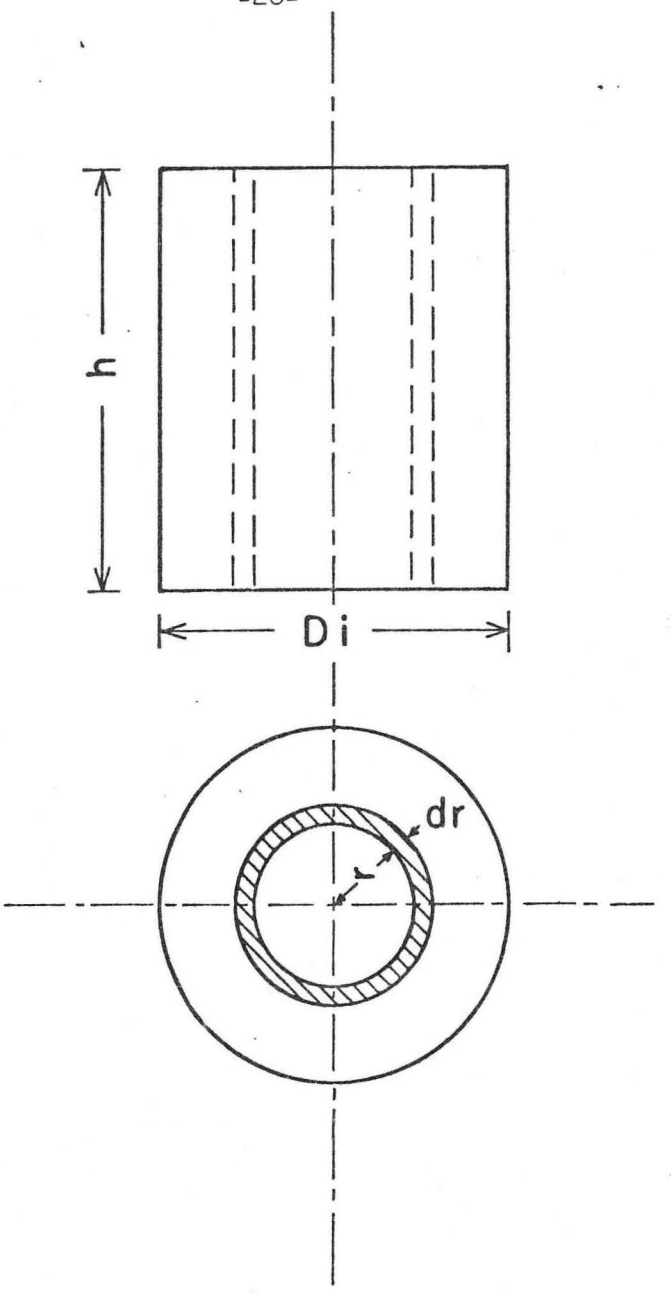

MUB-10367

Fig. 6. Calculation of centrifugal pressure, P_c.

$$P_c = \frac{\rho\omega^2 D_i^2}{8g_c} \tag{68}$$

For our rotor and fluid system

$$P_c = 4.63\times10^{-6}\ N^2 \tag{69}$$

where P_c is in psi and N is in rpm

5. Centrifugal Pressure Loss Factor

When the rotor is rotating and liquid flows through the membrane it is observed that the total pressure P on the liquid in the outer cylinder is given by

$$P = \Delta P_{cl} + P_{ll} + P_c + \Delta P + P_0 \tag{70}$$

where P = pressure in outer cylinder

ΔP_{cl} = centrifugal pressure loss

ΔP_{ll} = pressure loss in liquid lines

P_0 = discharge pressure (atomospheric pressure in this case)

P_c = centrifugal pressure

ΔP = effective pressure drop across the membrane and cake

ΔP_{cl} is quite analogous to the unrecoverable pressure loss in a venturi. Liquid enters the filter chamber at the bottom and is accelerated to an angular velocity equal to that of the rotor. However, the whole kinetic energy is not recovered when the filtrate leaves the rotor. ΔP_{cl} depends on the filtration rate Q and the rpm N. A loss factor ϕ is defined as

$$\phi = \frac{\Delta P_{cl}}{\Delta P_{cl} + P_c} \tag{71}$$

D. Cake Thickness Calculation

As filtration proceeds the cake thickness L increases. It is not convenient to measure L as a function of time. However an equation can be developed to calculate L as a function of θ for a constant pressure filtration. From Eq. (16):

$$\text{at } \theta = 0 \qquad R_0 = \frac{\Delta P}{q_0} \tag{72}$$

$$\text{at } \theta = \theta \qquad R = \frac{\Delta P}{q} \tag{73}$$

and

$$\frac{R}{R_0} = \frac{q_0}{q}$$

Combining this relation with Eq. (17):

$$L = \frac{R_0}{\beta} \quad \frac{q_0 - q}{q} \tag{74}$$

IV. DESCRIPTION OF THE EQUIPMENT, MEMBRANE AND SLURRY

A. Equipment

The flowsheet of the experiment has been briefly described in Chapter II. Figure 7 shows an over-all view of the equipment. The slurry tank is made of stainless steel and was designed for 100 psig. It is 20 in. in diam and 24 in. high and can store about 100 liters of slurry. It is baffled and is provided with a 4 in. impeller runing at about 600 rpm. This keeps the slurry in uniform suspension. A level gauge indicates the slurry level in the tank. A 1/2 in. pipe connects the slurry tank to the filter chamber. Figure 9 shows a detailed drawing of the filter chamber assembly. The filter chamber is made of stainless steel and designed for 100 psig. Two rotary Crane seals were used. Details of these seals and bearing assemblies are given in Figs. 10 and 11. In these Crane seals a graphite ring, attached to the shaft rotates on a stationary ceramic ring. A joint was provided in the lower half of the shaft to remove the whole filter membrane assembly from the filter chamber to replace the membrane. Figure 8 shows the rotor removed from the filter chamber.

The rotor is driven by a 3 phase Z flow-type Reeves variable speed motor of 1.5 hp. The motor speed can be easily varied from 420 to 4200 rpm by turning a wheel and stays constant without any control or adjustment. A Weston tachometer was installed to measure the rpm. Power input to the motor was measured by the two wattmeter method. Electrical connections for the wattmeters are shown in Fig. 12.

Pressure in the filter chamber was measured by a standard pressure gauge 0- 60 psig reading up to 0.2 psi. The pressure tap consists of a cylindrical tube 1/4 in. o.d. and 1/8 in. i.d. with a 1/8 in. diam hole, placed 1/8 in. away from the membrane surface. The tap hole was oriented to avoid the impact of the rotating liquid mass. Thus, static pressure was measured by the pressure gauge. This was checked by completely closing the filtrate exit valve and pressurizing the system to about 10 psig. When the motor was started the pressure reading did not change.

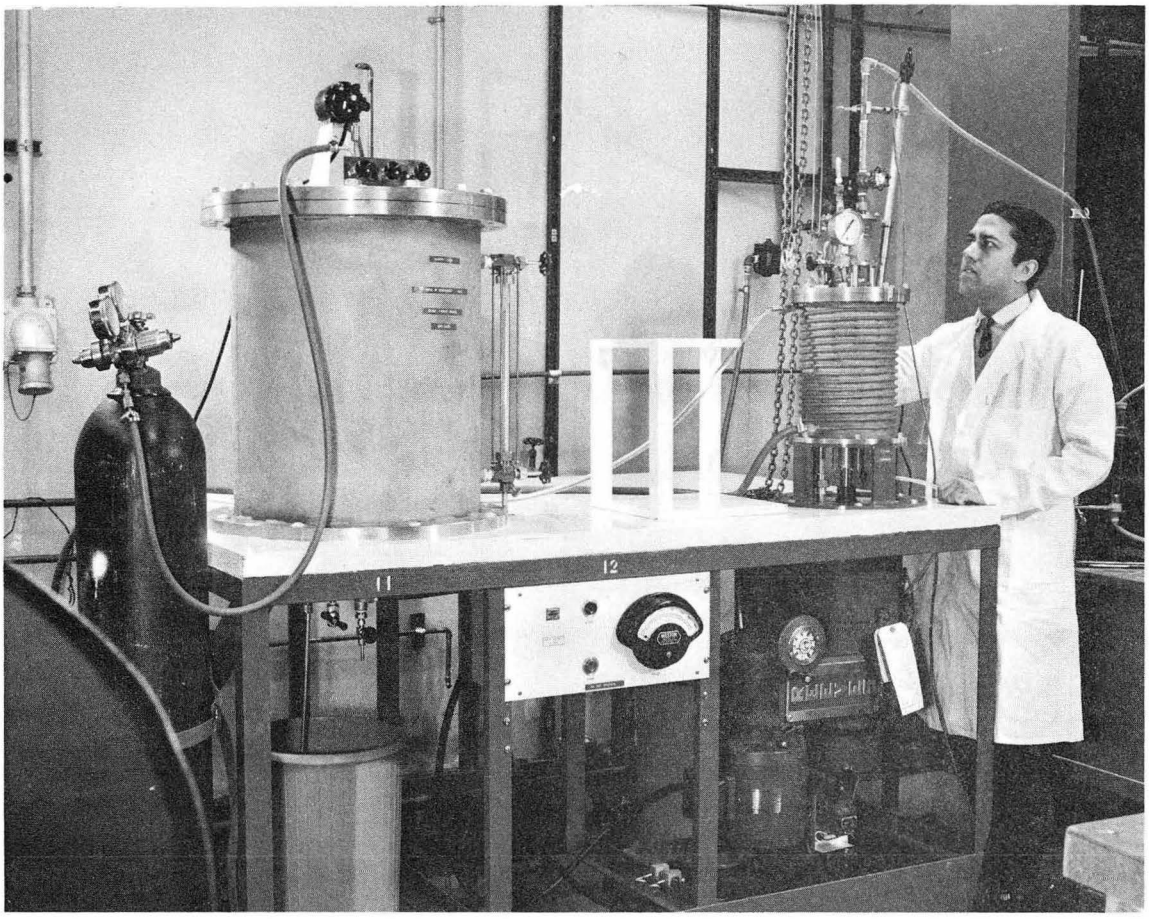

ZN-5995

Fig. 7. Overall view of the equipment.

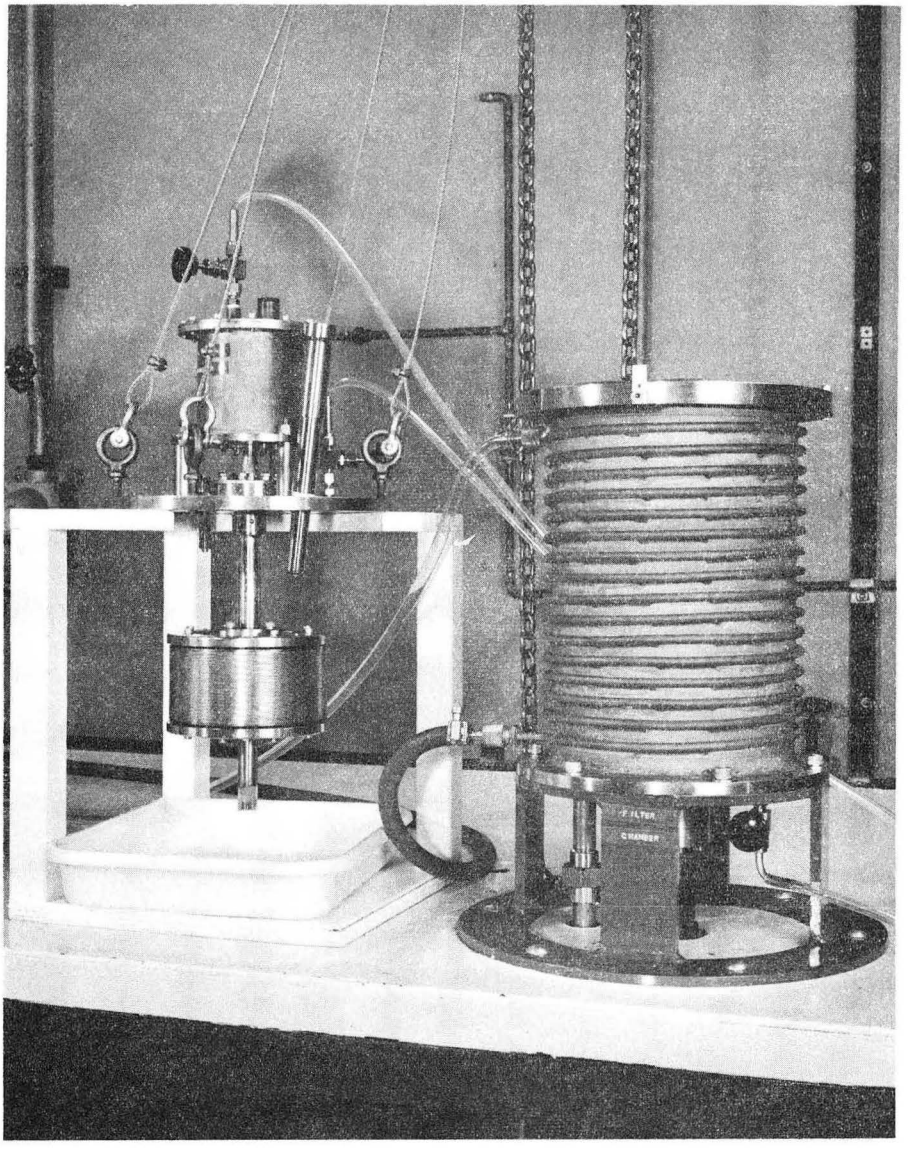

ZN-5994

Fig. 8. Detailed view of the filter chamber, rotor, and filtrate chamber. Rotor is shown removed from the filter chamber.

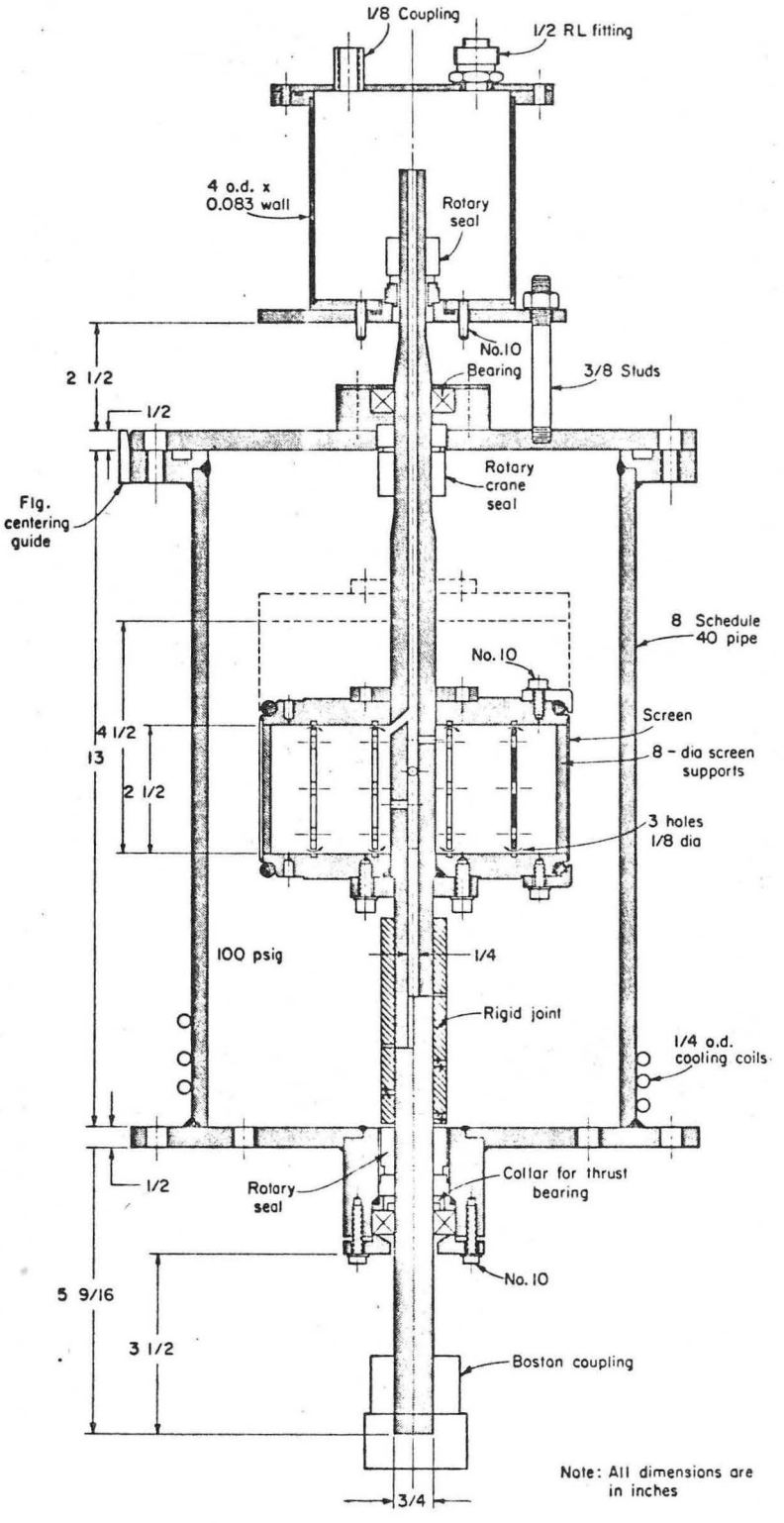

Fig. 9. Detailed engineering drawing of the filter assembly.

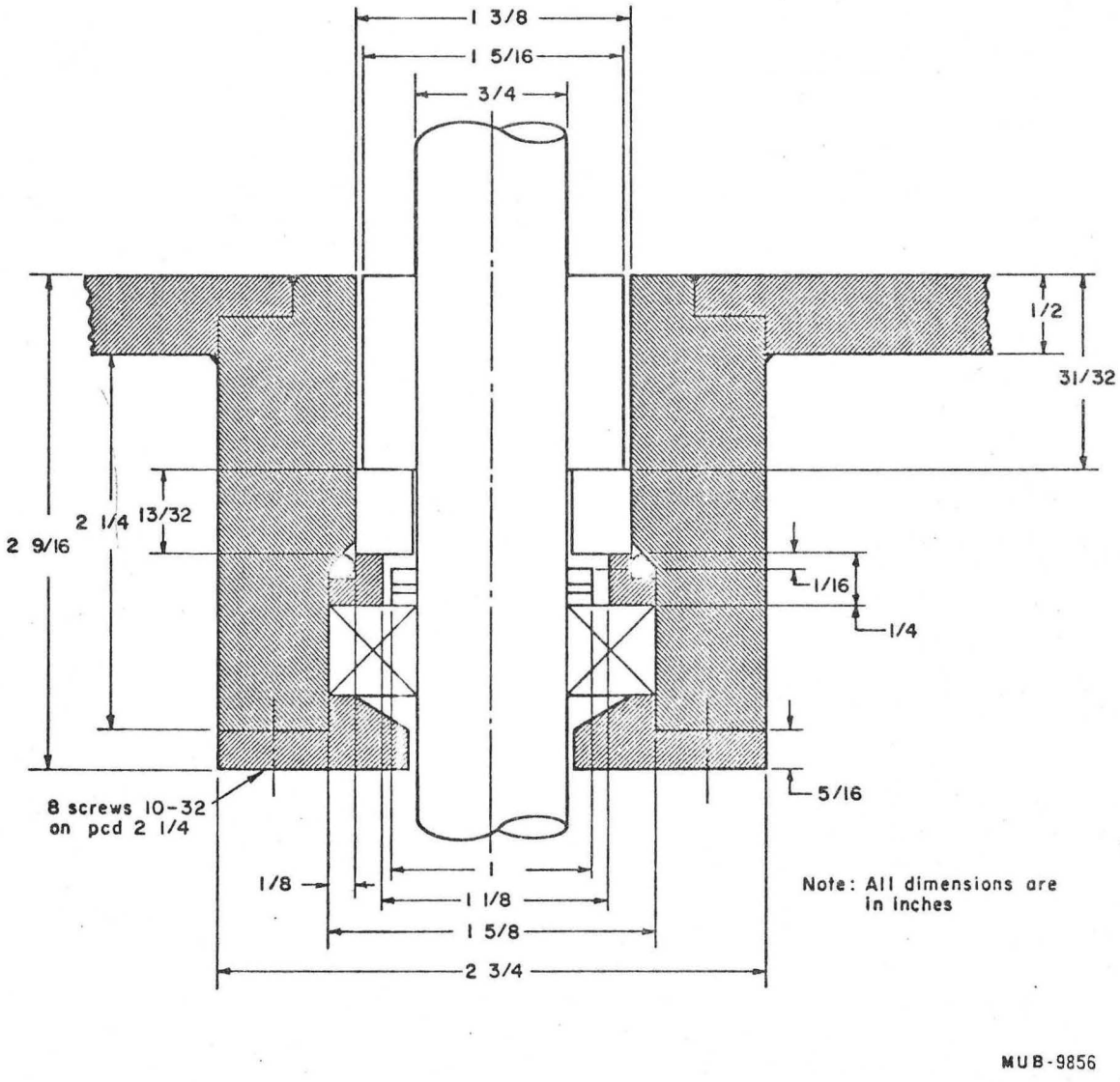

Fig. 10. Details of the lower seal and bearing.

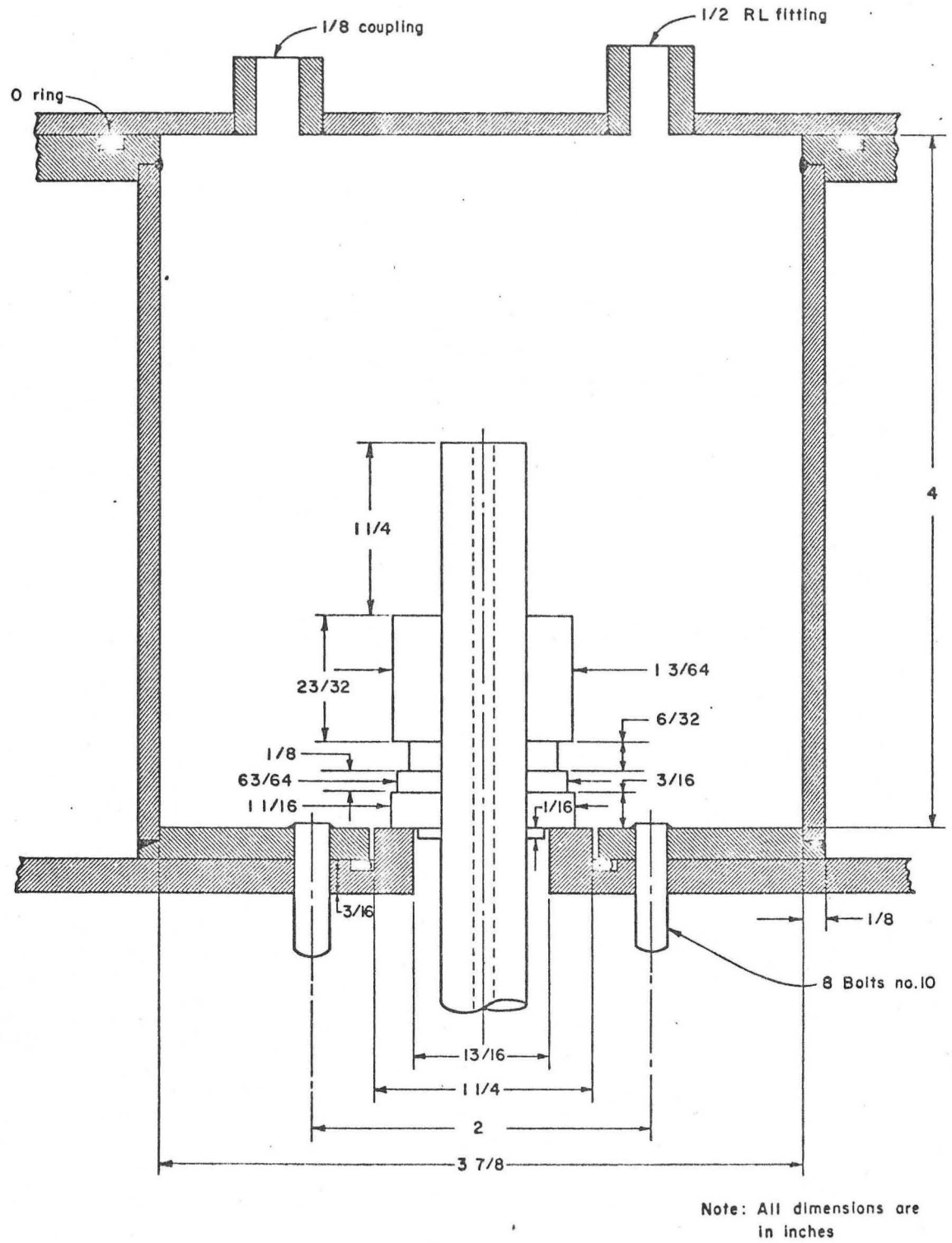

Fig. 11. Details of the top seal.

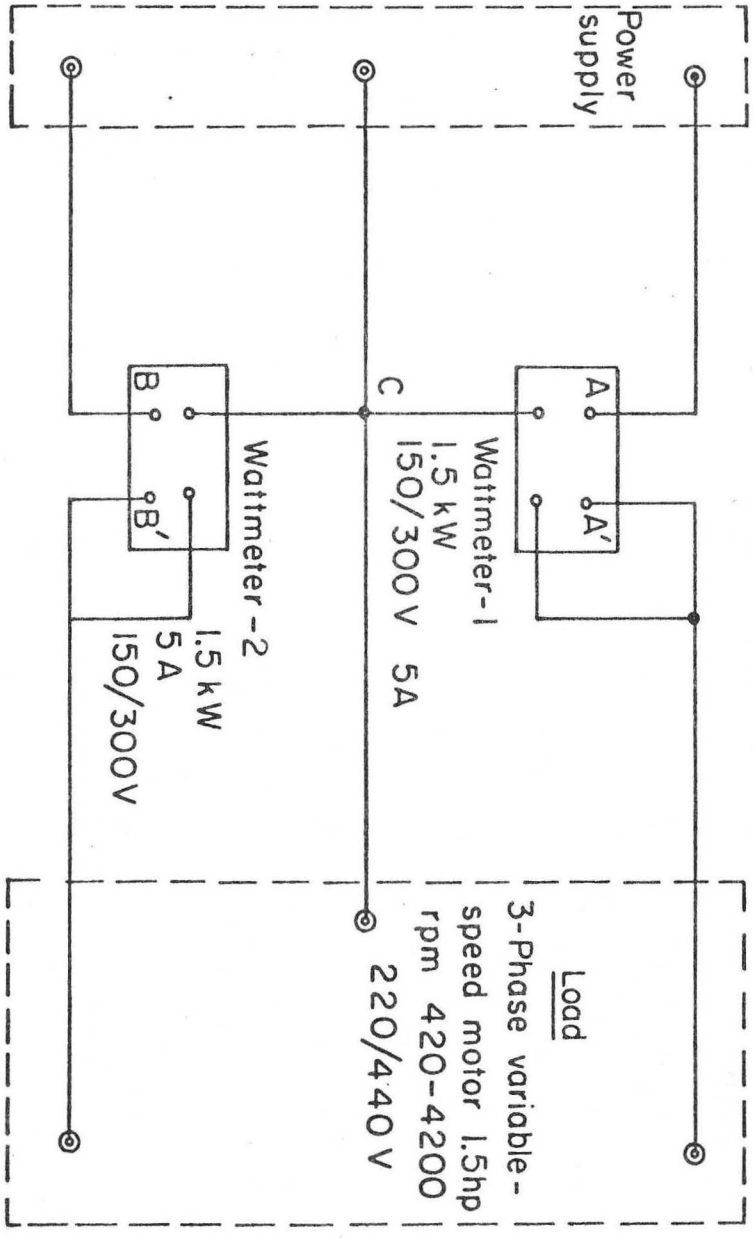

Fig. 12. Circuit diagram for power measurement in 3 phase motor.

The flow of filtrate was measured by two rotameters 35/70 ml/sec and 150 ml/sec connected in parallel. Smaller flow rates were measured by collecting filtrate in a graduated cylinder for 10 or 20 seconds.

The temperature of the slurry in the filter chamber was controlled at 25°C. A thermometer was kept in a thermometer well in the slurry chamber and was connected to an on-off temperature controller which opened or closed the solenoid valve on the cooling coils. 1/4 in. o.d. stainless steel tubes were welded on to the outside of the filter chamber to provide a cooling capacity of about 13 cals/sec for each °C of driving force. A small shell and tube type heat exchanger was also used to initially heat or cool the slurry to 20 - 24 °C so that the temperature of the slurry in the filter chamber could be easily controlled at 25°C.

B. Filter Membranes

The filter membranes were manufactured by Millipore Filter Corporation, Bedford, Massachusetts. Millipore filters are porous structures of pure biologically inert cellulose esters. These membranes have uniform pore sizes of about 80% porosity. Two grades of microweb filter membranes were selected for these experiments. Their properties are given in Table I.

Table I. Properties of the microweb Millipore membranes.

Grade	Mean pore diam (μ)	Standard deviation of pore size distribution. (μ)	Thickness (μ)
WS	3.0	±0.9	150 ± 10
WH	0.45	±0.02	150 ± 10

C. Slurries

It was desired to have a slurry of spherical particles of very uniform diam. Two kinds of polymer latex were obtained from the Dow Chemical Co., Midland, Michigan. Their properties are given in Table II.

Table II. Properties of polystyrene latex.

Property	Poly styrene latex	Styrene divinylbenzene copolymer latex
Particle diam	1.305 μ	6 - 14 μ
Standard deviation of particle size distribution.	0.0158 μ	.....
Density (g/cc)	1.056	1.056
% solids	10	10

These slurries were diluted with distilled water to get about 60 - 100 liters of slurry containing 0.5 - 1.0 g/liter of solids. Figures 13 and 14 show the particles in these slurries. The following two sysems of slurries and membranes were used:

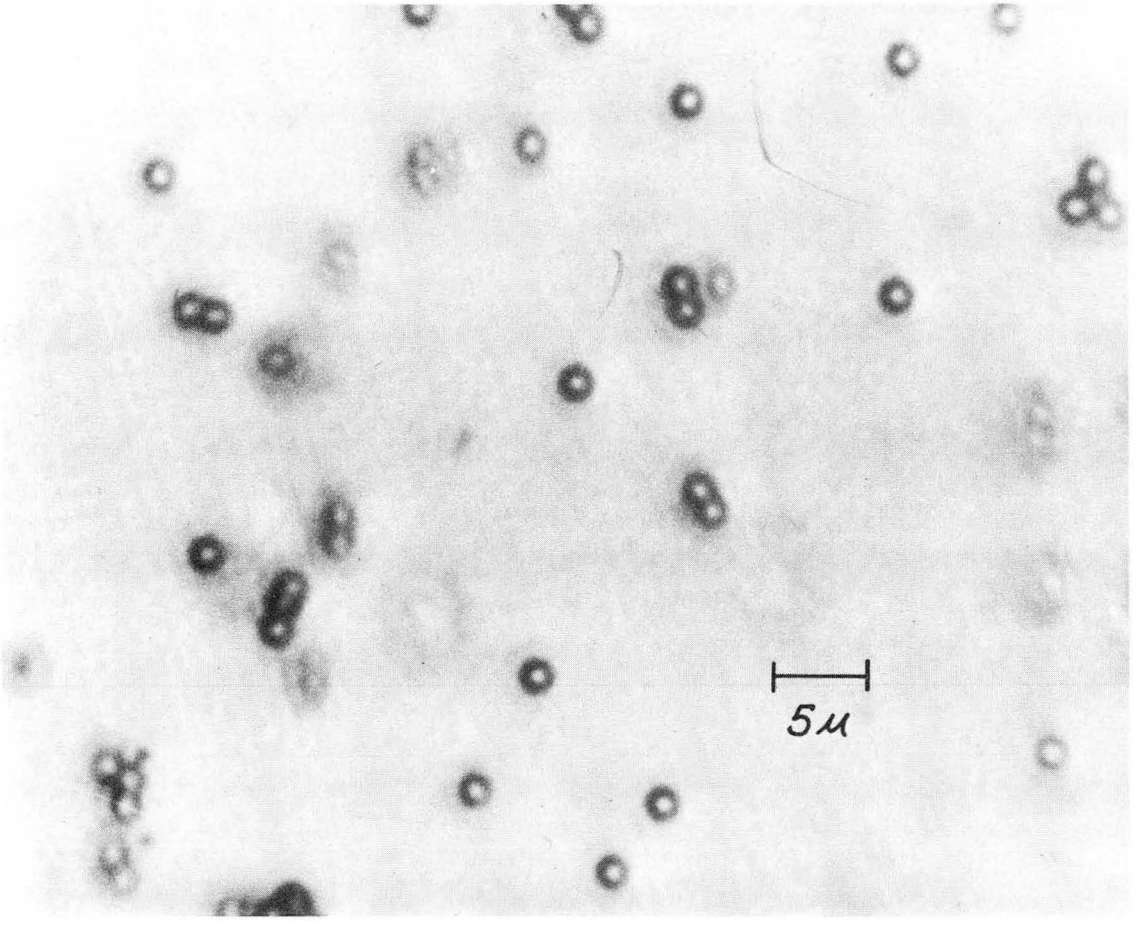

ZN-5996

Fig. 13. Spherical particles of polystyrene ×2000, mean diam = 1.305 μ.

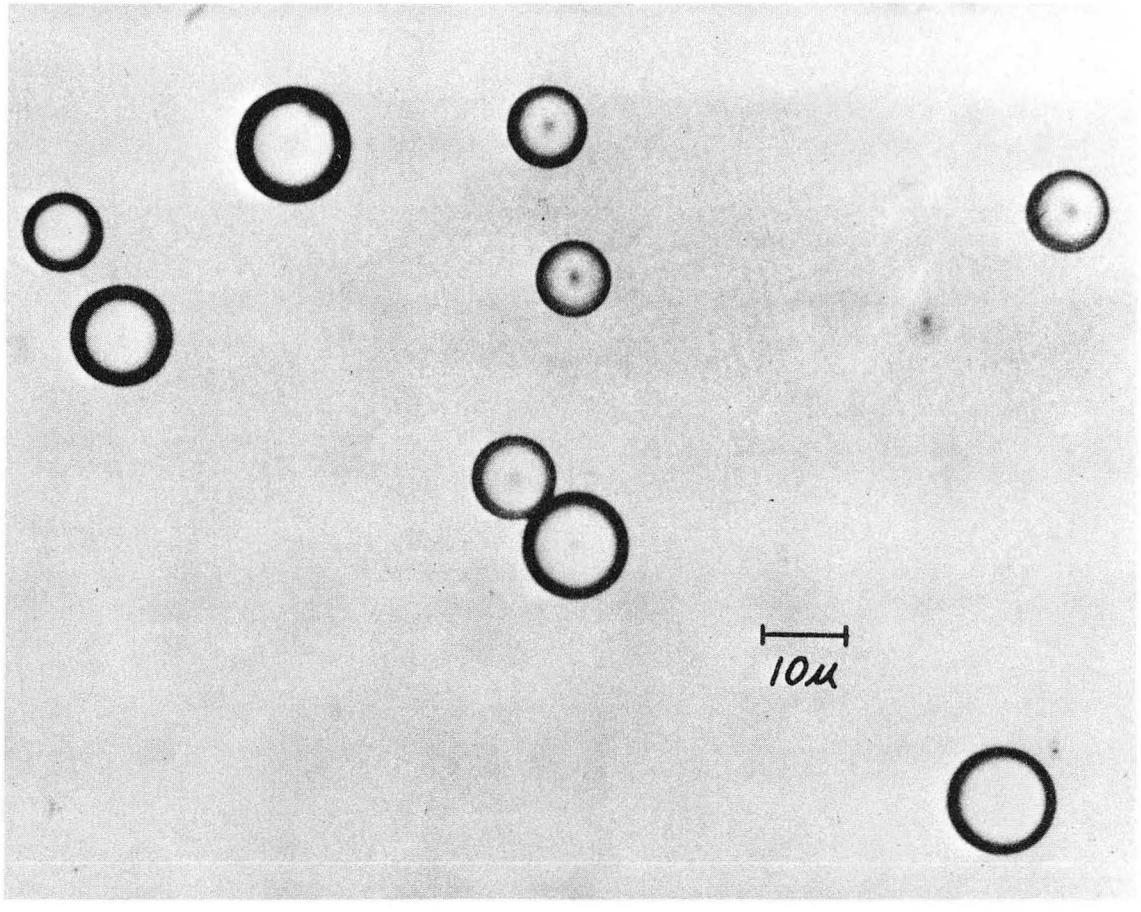

ZN-5997

Fig. 14. Spherical particles of styrene divinyl benzene copolymer latex ×980 particles diam 6 - 14 μ.

1. Millipore microweb grade WH membrane and 1.3 μ mean particle diam polystyrene latex.
2. Millipore microweb grade WS membrane and 6 - 14 μ particle diam and styrene divinyl benzene copolymer latex.

V. EXPERIMENTAL PROCEDURE AND DATA

A. Pressure Measurements

1. Centrifugal Pressure Measurement

Equation (70) gives the total pressure required to get a flow through the rotating membrane. If the rotor is rotating without membrane and the flow approaches zero, we have

$$\Delta P_{cl} = \Delta P_{ll} = \Delta P = 0$$

and

$$P = P_c$$

To determine centrifugal pressure P_c experimentally, the rotor (without membrane) was run at a constant rpm and the valve at the slurry inlet to the filter chamber was slowly closed until there was no flow of water through the rotor and the pressure reading was taken. Temperature was controlled at 25°C. The data for P_c at different rpm are given in Table III and are plotted in Fig. 15. P_c is experimentally given by Eq. (75).

$$P_c = 4.72 \times 10^{-6} N^2 \qquad (75)$$

where P_c is in psi and N is rpm.

This result compares favorably with the theoretical relation Eq. (69)

Table III. P_c for water at 25°C using 6 in. diam rotor.

N (rpm)	P_c(psi)
500	1.0
600	1.6
700	2.2
800	3.0
1000	4.8
1200	6.8
1500	10.6
1800	15.0
2000	18.6
2200	22.4
2400	26.4

2. Measurement of Pressure Loss in Liquid Lines (ΔP_{ll})

Water was allowed to flow through the stationary rotor without membrane and pressure readings were taken for different flow rates. The data are given in Table IV and are plotted in Fig. 16. ΔP_{ll} did not change when a nylong cloth was wrapped around the rotor.

3. Measurement of Centrifugal Pressure Loss (ΔP_{cl})

The total pressure P was measured for different flow rates through the rotor (without the membrane) at various values of N. P_c and ΔP_{ll} were obtained from Figs. 15 and 16 and Eq. (70) was used to calculated ΔP_{cl} ($\Delta P = 0$). The experimental data for ΔP_{cl} is given in in Table V. Fig. 17 shows ΔP_{cl} as a function of Q for different N. The data from Fig. 17 is replotted in Fig. 18 to show the dependence of P_{cl} on N for a constant Q. This data is given in Table VI. The lines in Fig. 18 are all parallel with a slope of 1.3. Expressing ΔP_{cl} as

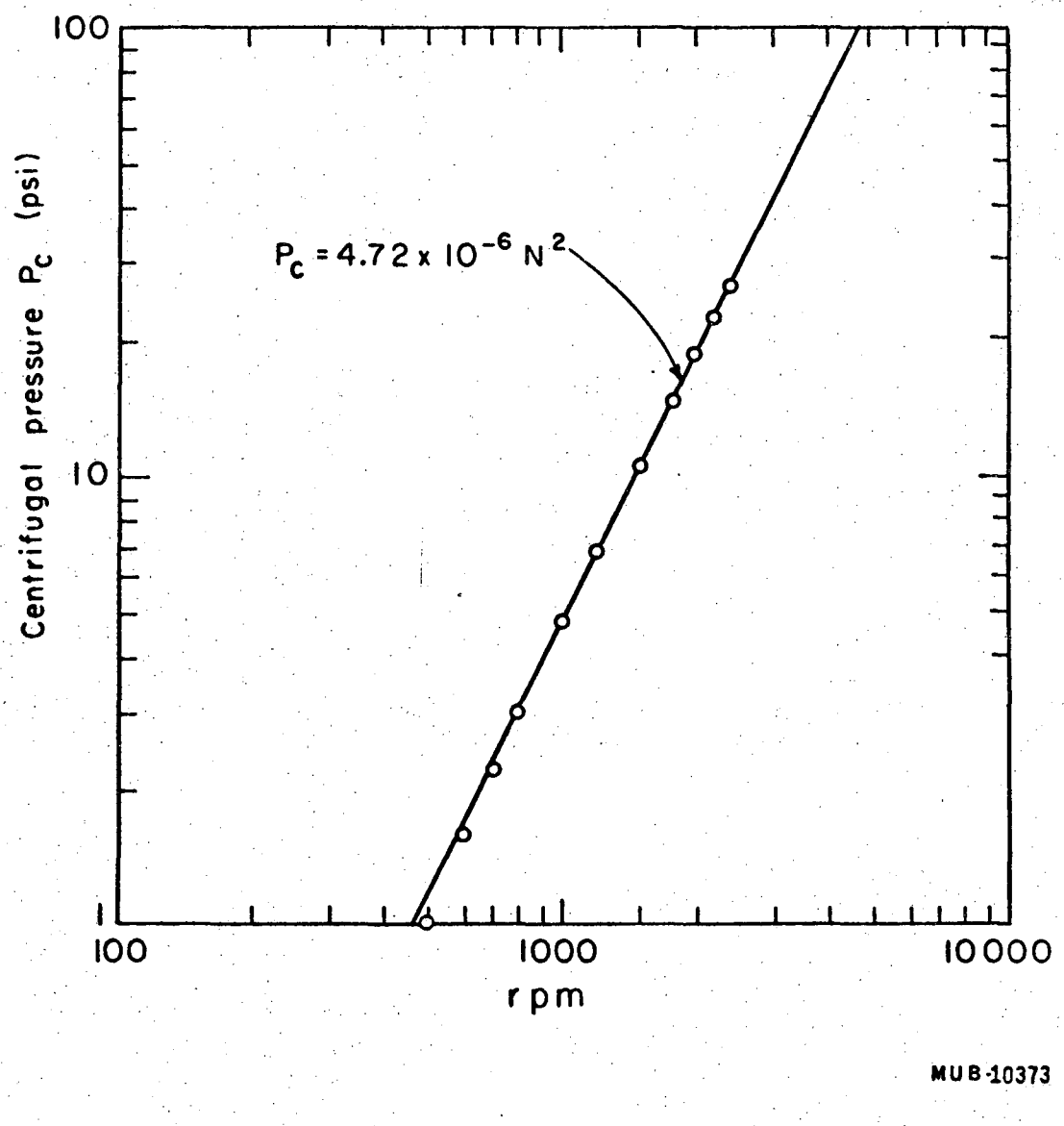

Fig. 15. Centrifugal pressure P_c vs rpm for water at 25°C and rotor diam = 6 in.

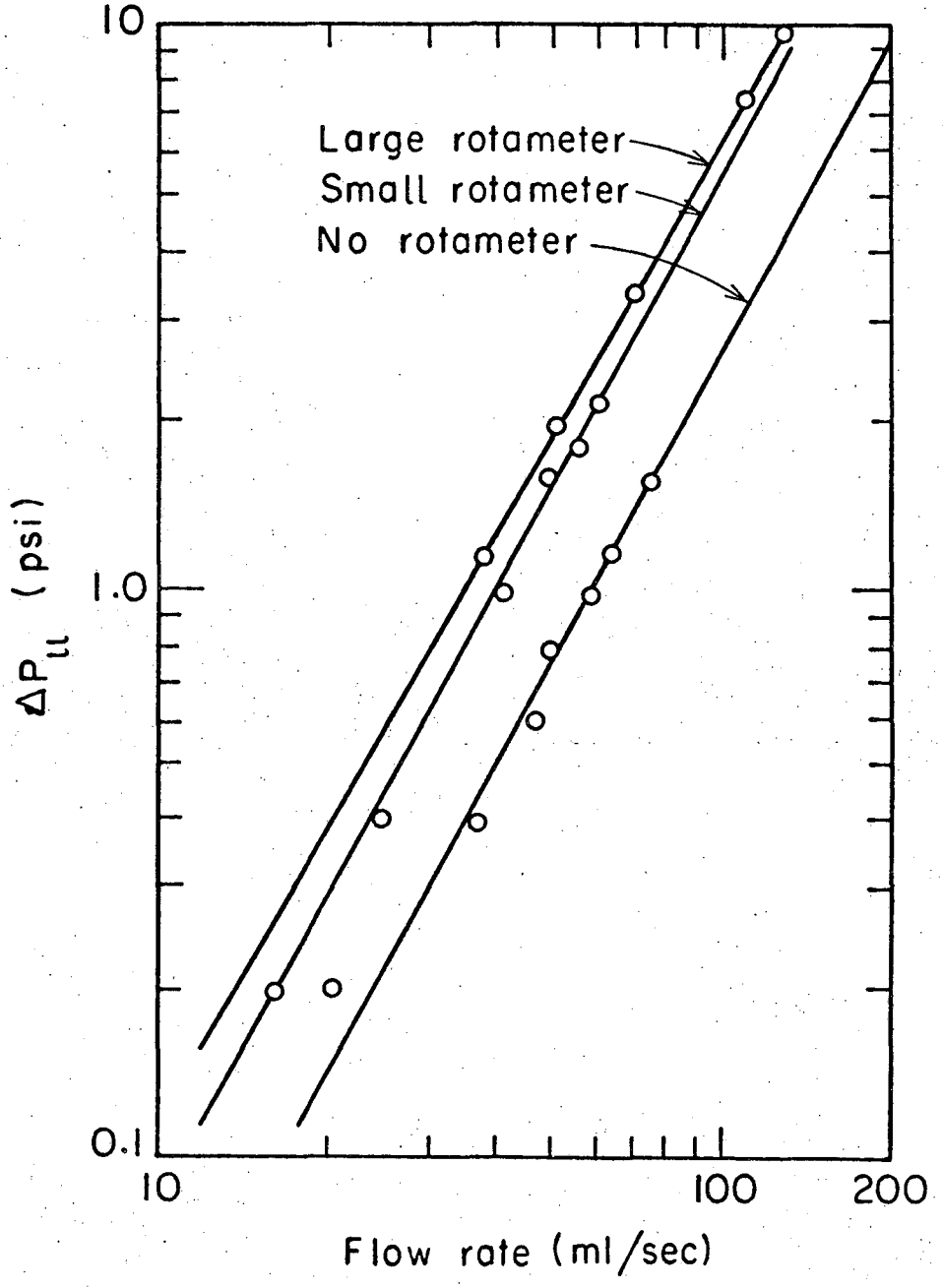

Fig. 16. Pressure drop in liquid lines vs flow rate for water at 25°C.

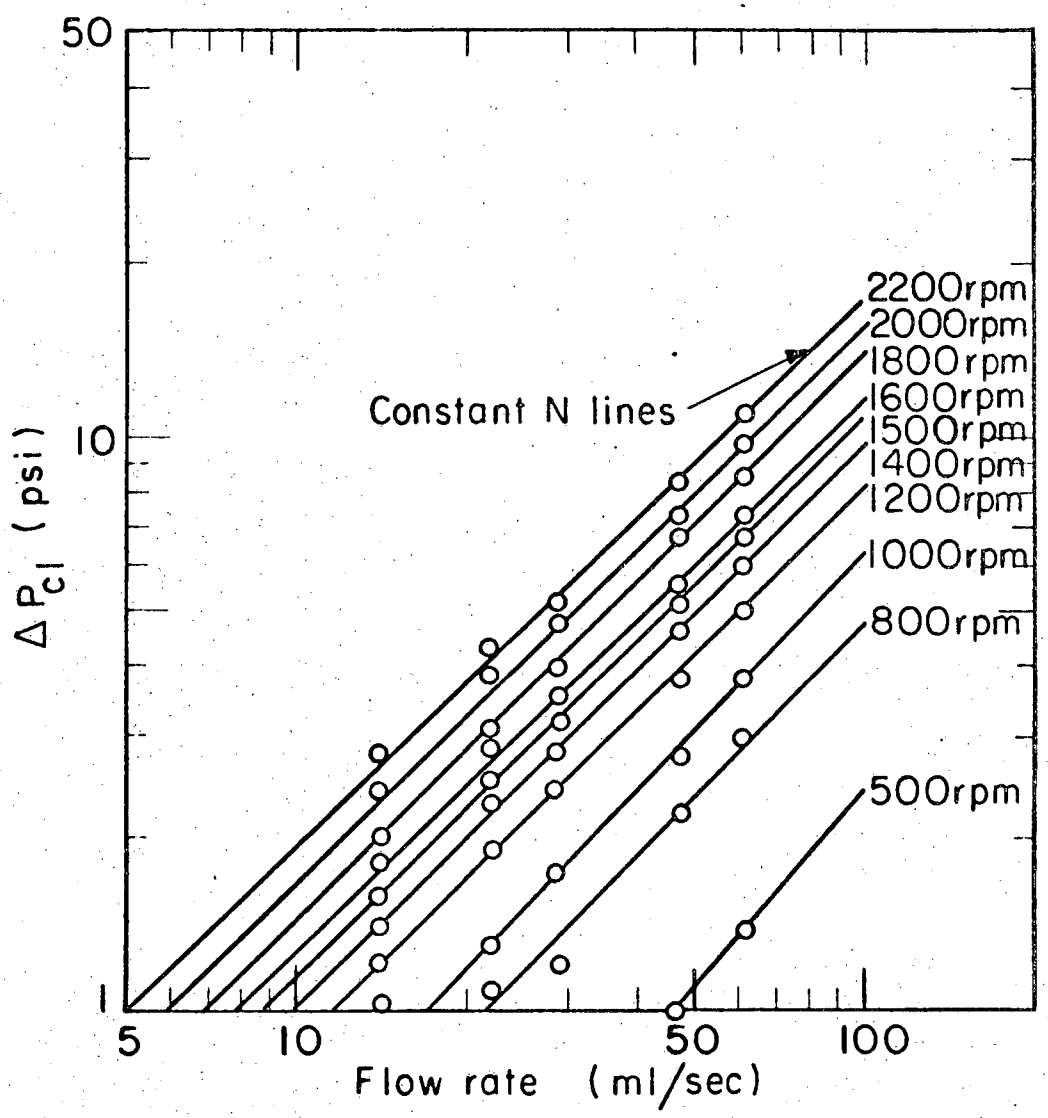

Fig. 17. Centrifugal pressure loss vs flow rate at constant rpm.

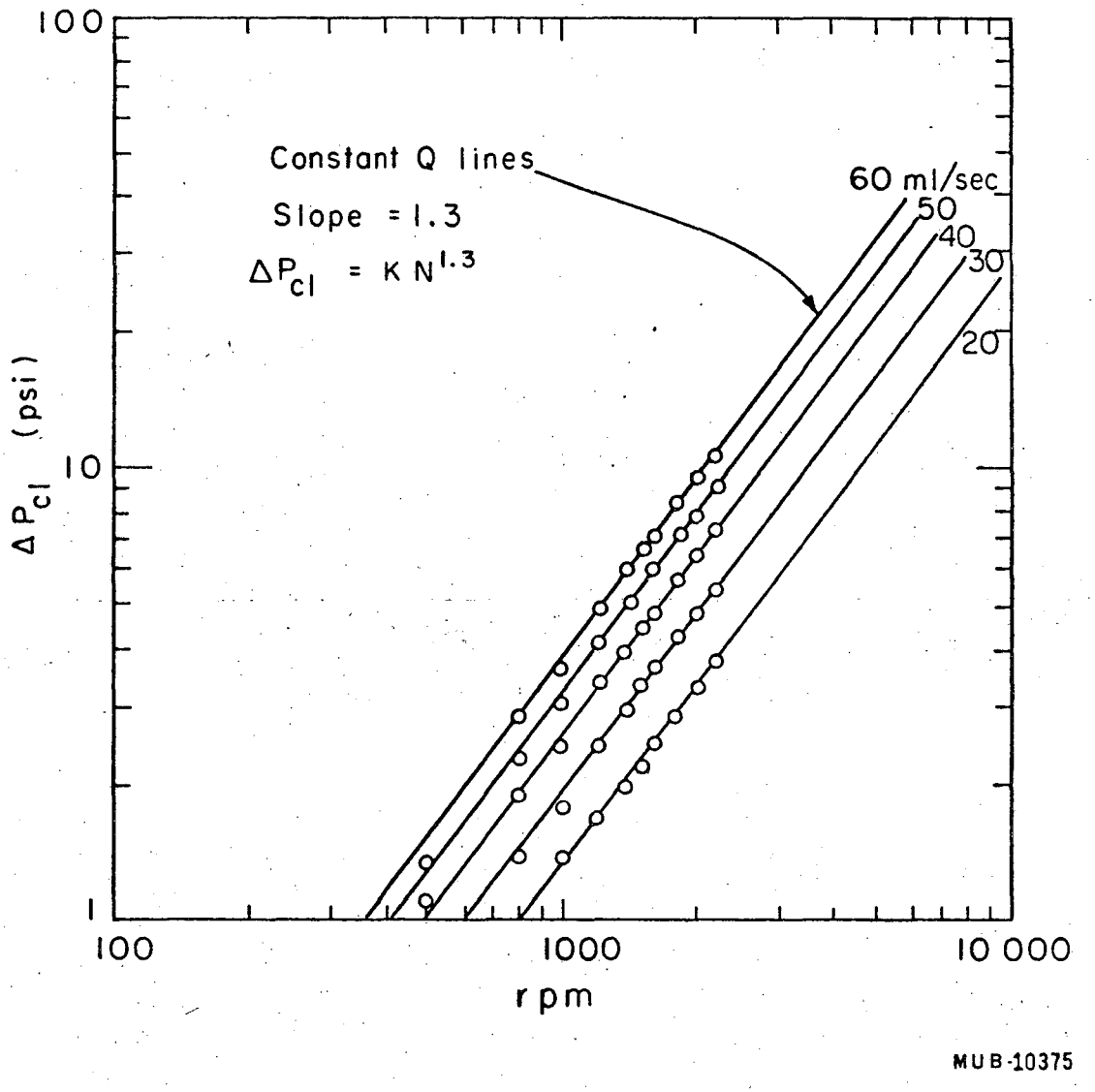

Fig. 18. Centrifugal pressure loss vs rpm at constant flow rate as obtained from Fig. 17.

Table IV. ΔP_{11} for water at 25°C at different Q.

Small rotameter		Large rotameter		No rotameter	
Q (ml/sec)	ΔP_{11} (psi)	Q (ml/sec)	ΔP_{11} (psi)	Q (ml/sec)	ΔP_{11} (psi)
16	0.2	38	1.2	21	0.2
25	0.4	52	2.0	37	0.4
41	1.0	70	3.4	47	0.6
50	1.6	112	7.6	50	0.8
56	1.8	130	9.8	59	1.0
60	2.2			65	1.2
				74	1.6
				82	1.8

$$\Delta P_{cl} = K N^{1.3} \tag{76}$$

where P_{cl} is in psi and N is in rpm.
The constant K was calculated for different Q and is given in Table VII. Figure 19 shows K as a function of Q.

$$K = 1.0 \times 10^{-5} Q^{0.95} \tag{77}$$

The total filtering area = 364 cm^2

$$K = 2.75 \times 10^{-3} q^{0.95} \tag{78}$$

From Eqs. (76) and (78) we can express ΔP_{cl} empirically as

$$\Delta P_{cl} = 2.75\ 10^{-3} q^{0.95} N^{1.3} \tag{79}$$

where ΔP_{cl} = psi
q = ml/sec cm^2
N = rpm

Equation (79) fits the experimental data within 5% for q up to 0.16 ml/sec cm^2. However it was observed that for higher flow rates ΔP_{cl} was much smaller than the calculated values from Eq. (79)

The centrifugal pressure loss factor ϕ is defined by Eq. (71). Substituting for P_c and ΔP_{cl} from Eqs. (69) and (79) respectively we get

$$\phi = \frac{1}{1 + 1.72 \times 10^{-3} \frac{N^{0.7}}{q^{0.95}}}$$

The above equation empirically gives ϕ for a rotor of 6 in. diam with water flow rates less than 0.165 ml/sec cm^2.

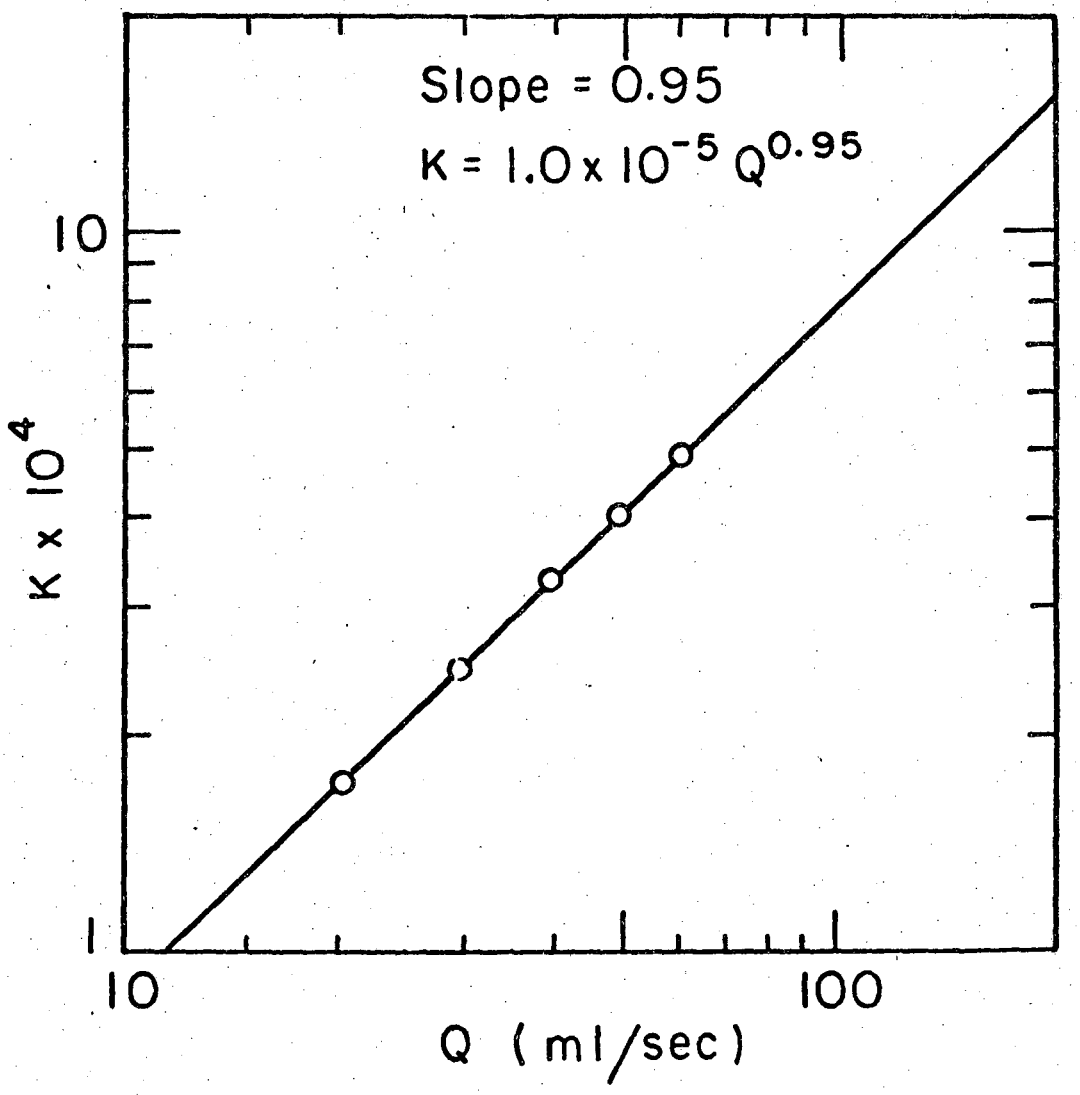

Fig. 19. K vs Q as obtained from Fig. 18.

Table V. ΔP_{cl} for water at 25°C at various Q and N.

N (rpm)	ΔP_{cl} (psi)				
	Q=14 (ml/sec)	Q=22 (ml/sec)	Q=29 (ml/sec)	Q=47 (ml/sec)	Q=61 (ml/sec)
500	0.6	0.7	0.8	1.0	1.4
800	0.8	1.1	1.2	2.2	3.0
1000	1.0	1.3	1.8	2.8	3.8
1200	1.2	1.9	2.4	3.8	5.0
1400	1.4	2.3	2.8	4.6	6.0
1500	1.6	2.5	3.2	5.2	6.8
1600	1.8	2.9	3.6	5.6	7.2
1800	2.0	3.1	4.0	6.4	8.6
2000	2.4	3.9	4.8	7.4	9.8
2200	2.8	4.3	5.2	8.4	11.0

Table VI. ΔP_{cl} data as read from Fig 17.

N (rpm)	ΔP_{cl} (psi)				
	Q=20 (ml/sec)	Q=30 (ml/sec)	Q=40 (ml/sec)	Q=50 (ml/sec)	Q=60 (ml/sec)
500	-	-	-	1.1	1 35
800	-	1.4	1.9	2.3	2 85
1000	1.4	1.8	2.45	3.1	3.7
1200	1.7	2.5	3.4	4.2	5.0
1400	2.0	3.0	4.0	5.0	6.0
1500	2.25	3.4	4.5	5.6	6.7
1600	2.5	3.7	4.8	6.0	7.2
1800	2.85	4.3	5.7	7.1	8.5
2000	3.3	4.9	6.4	8.0	9.6
2200	3.8	5.5	7.4	9.1	10.7

Table VII. Data for K from Fig. 18.

Q (ml/sec)	$K \times 10^4$
20	1.7
30	2.44
40	3.32
50	4.06
60	4.87

B. Power Measurements and Drag Coefficient

Power input to the motor was measured by two wattmeters as shown in Fig. 12. Power input to the motor was measured at different rpm with the rotor in air and in water. The difference of these two readings gives the power loss due to water friction. Two similar rotors of 6 in. diam and 3 in. and 5 in. high were used. It was observed that at a given rpm power loss due to water friction depends on the system conditions. In the first case the filtrate outlet valve was closed and the slurry in the filter chamber was at 35 psig and in the second case the filtrate outlet valve was open and there was a small flow of water (0.05-0.1 ml/sec cm^2) through the rotor. Power loss due to fluid friction was less for the second case at the same rpm. However this difference was not a function of the flow rate. The experimental data are given in Table VIII. The data for power loss due to water friction with a small flow for both the rotors are plotted in Fig. 20. Table IX gives the difference of power loss due to water friction for the two rotors at the same rpm as read from Fig. 20. This difference is the power loss due to water friction on the rotor surface 2 in. in height. This power loss P_τ (power loss due to shear stress on the rotor surface of 2 in. height, total area = 243 cm^2). is plotted in Fig. 21 and is given by

$$P_\tau = 3.8\times10^{-11}N^{3.9} \tag{80}$$

where P_τ is in watts.

If τ_w is the shear stress on the membrane surface in g_f/cm^2 from Eq. (80) we have

$$\tau_w = 2.01\times10^{-9}N^{2.9} \tag{81}$$

Table VIII. Experimental data for power loss due to fluid friction for water at 25°C for rotors of 6 in. diameter.

N (rpm)	Power loss due to water friction (watts) (difference of readings in water and air)			
	3 in. high rotor with small flow	5 in. high rotor		
		with small flow	no flow	% increase
1000	80	125	155	24
1200	155	205	230	12.2
1400	270	340	360	5.9
1500	345	400	455	13.7
1600	430	530	530	0.0
1800	600	740	790	6.8
2000	850	1060	1080	1.9
2200	1130	1510	1570	4.0
2300	1315	1730	1770	2.3

Table IX. Data for P_τ, τ_w, C_D and Re_D for our system.

N (rpm)	P_τ (watts)	v_0 (cm/sec)	τ_w (g_f/cm)	C_D	Re_D
1000	17	800	0.988	3.08×10^{-3}	6.81×10^{5}
1200	35	960		3.63×10^{-3}	8.18×10^{5}
1400	70	1120	2.66	4.15×10^{-3}	9.55×10^{5}
1500	90	1200		4.43×10^{-3}	10.20×10^{5}
1600	130	1280		4.70×10^{-3}	10.90×10^{5}
1800	170	1360	5.68	5.24×10^{-3}	11.60×10^{5}
2000	280	1600		5.74×10^{-3}	13.60×10^{5}
2200	400	1760		6.28×10^{-3}	15.00×10^{5}
2300	450	1840		6.53×10^{-3}	15.70×10^{5}
2500	630	2000		7.01×10^{-3}	17.00×10^{5}

using Eq. (64) we can get

$$C_D = 6.17\times10^{-6} N^{0.9} \qquad (82)$$

The data for P_τ, τ_w, C_D and Re_D are given in Table IX and are plotted in Fig. 22. to compare it with the work of Theodorsen and Regier.[18]

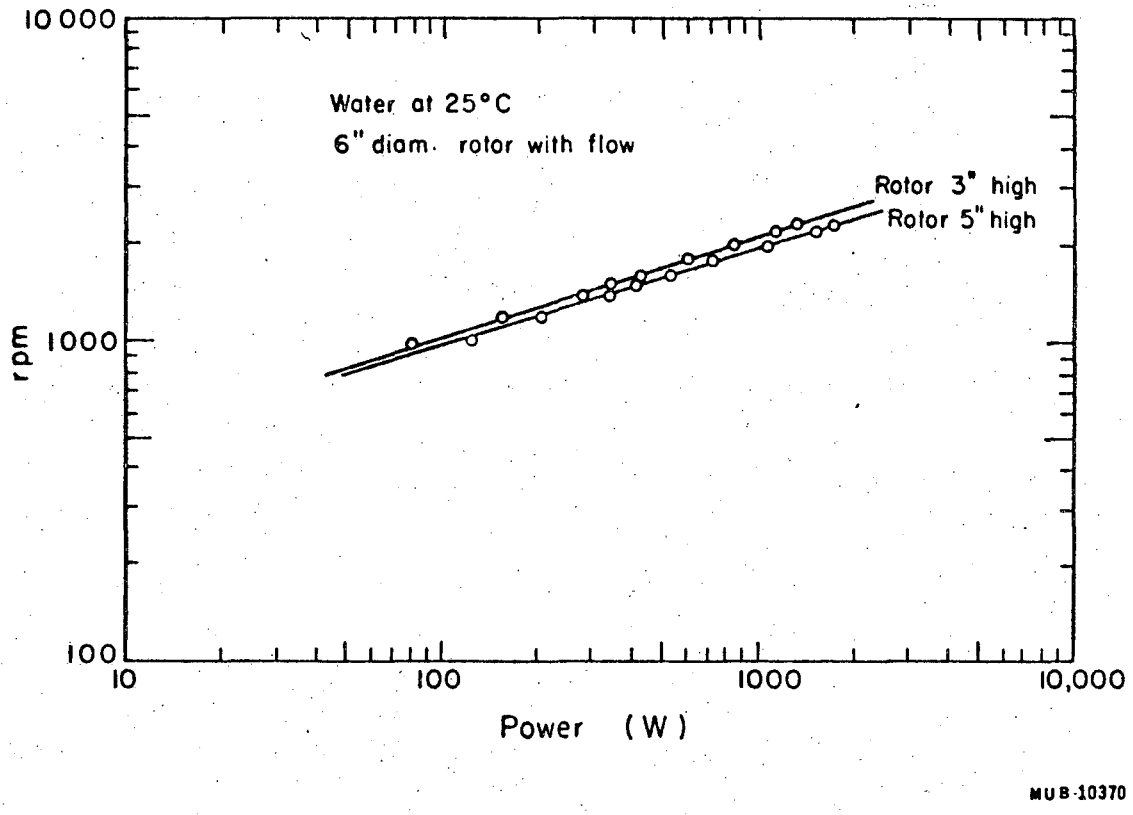

Fig. 20. Power loss due to water friction vs rpm at 25°C for rotor height of 3 in. and 5 in. Inner cylinder diam 6 in. and outer cylinder diam 8 in.

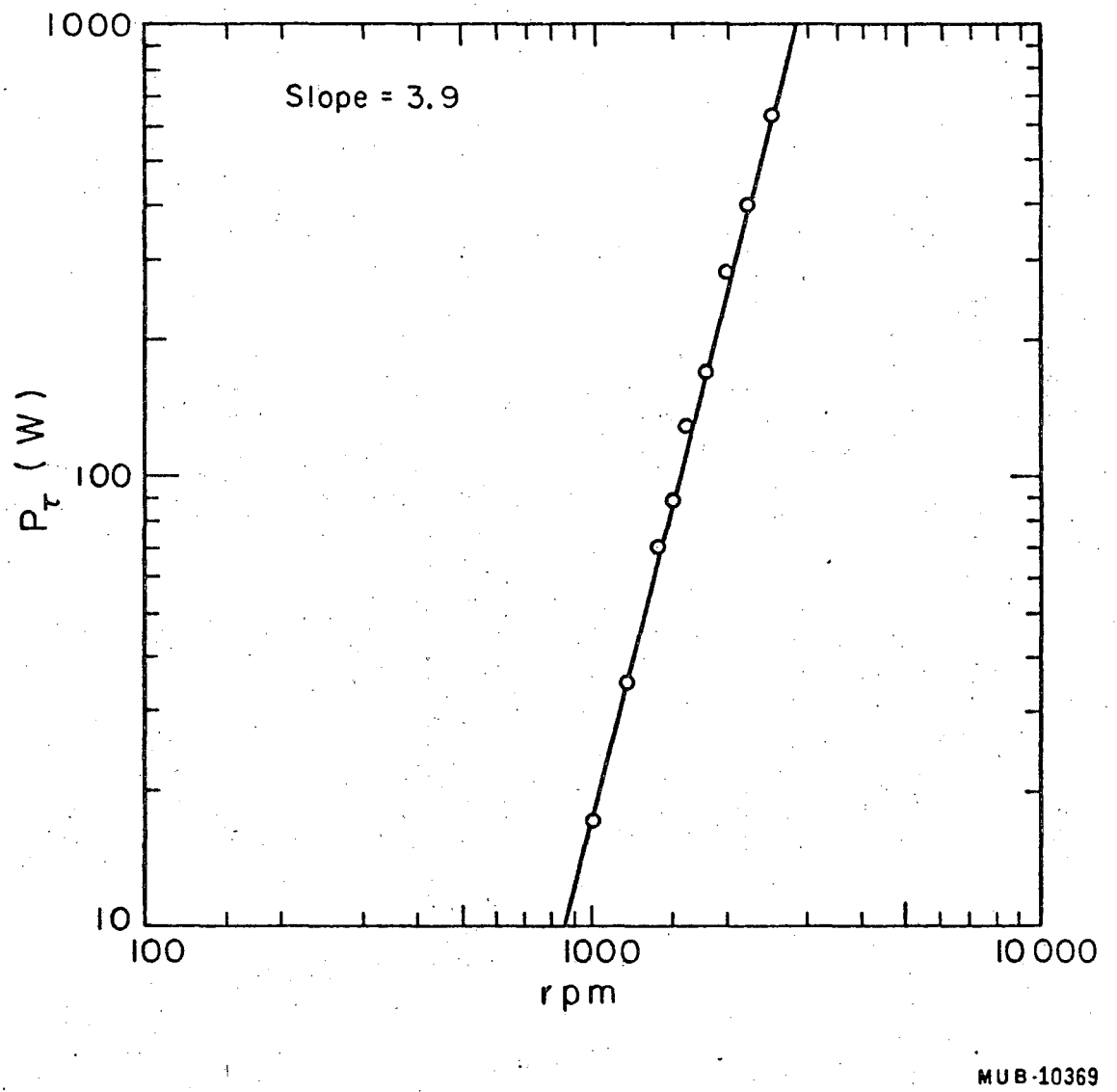

Fig. 21. Power loss due to water friction P_τ over area of 243 cm^2 vs rpm as obtained from Fig. 20.

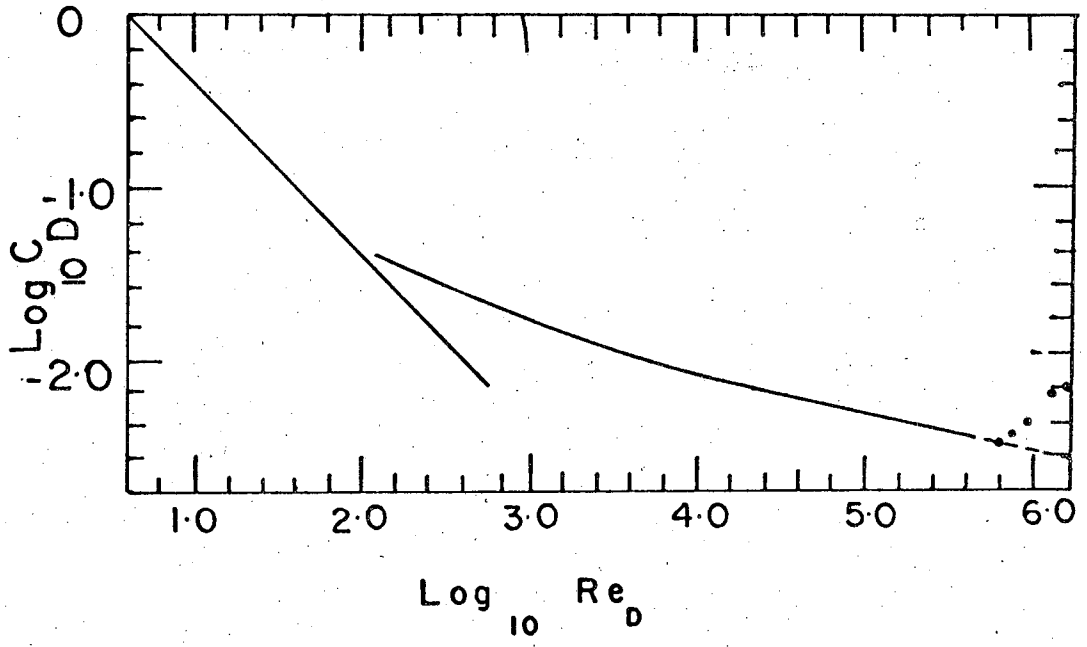

Fig. 22. Drag coefficient vs Re_D. Our data are compared with Theodorsen and Regier.[18]

C. Filtration Experiments Without Rotation

All experiments without rotation were done with Millipore Pyrex filter holder catalogue no. XX10-047-00. This is schematically shown in Fig. 23. It consists of a Pyrex glass funnel clamped onto a sinterd glass filter membrane support.

1. Flow of Clean Water Through the Membrane

Time for filtering 100 ml of clean distilled water (prefiltered through 0.22 μ membrane) through the membranes (0.45 μ and 3.0 μ) of 11.35 cm^2 filtering area at different vacuum was determined at 21°C. The data for q vs ΔP is shown in Fig. 24.

2. Incompressibility of the Cake

About 500 ml of 1.3 μ slurry (1 g/liter solids) was filtered through 0.45 μ membrane of 11.35 cm^2 filtering area. Time for filtering area. Time for filtering 50 ml of clean distilled water through this cake was determined at different vacuum. The resistance R was found to be 1010 g_f sec/ml for ΔP up to 10 psi, which shows that the cake is incompressible in this pressure range.

3. Porosity of the Cake

About 500 ml of slurry (1 g/liter solids) was filtered through the 0.45 μ membrane. Thickness of the wet cake was determined by a vertical traveling microscope. The cake was then dried and the weight of the dry cake determined. Knowing ρ_p, porosity of the cake was calculated

Porosity for 1.3 μ particles = 0.506

Porosity for 6-14 μ particles = 0.575

4. Additivity of the Cake Resistance

A known volume of slurry (10 or 20 ml) was filtered through the membrane to give a uniformly thin cake. The resistance R was then determined by determining the time of filtration for a known volume (50 or 100 ml) of clean distilled water through this cake. The cake resistance was determined after every addition of cake layer. At the

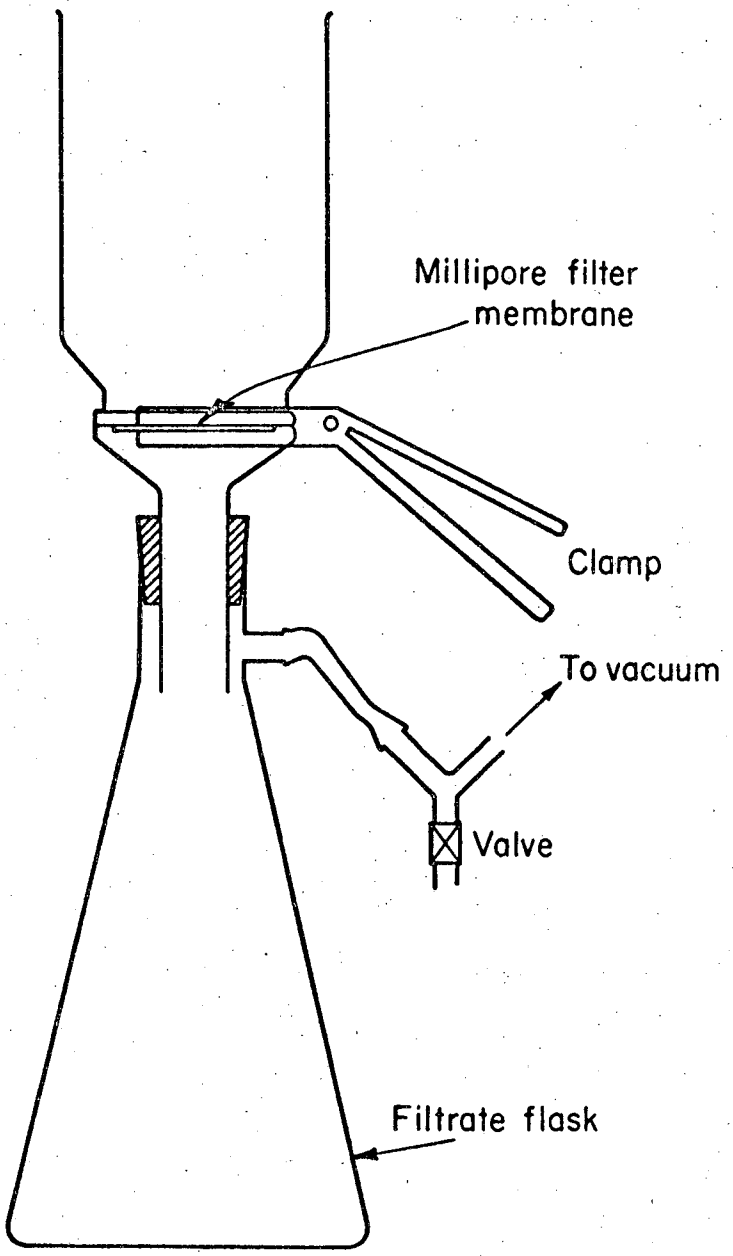

Fig. 23. Schematic view of Millipore filter holder.

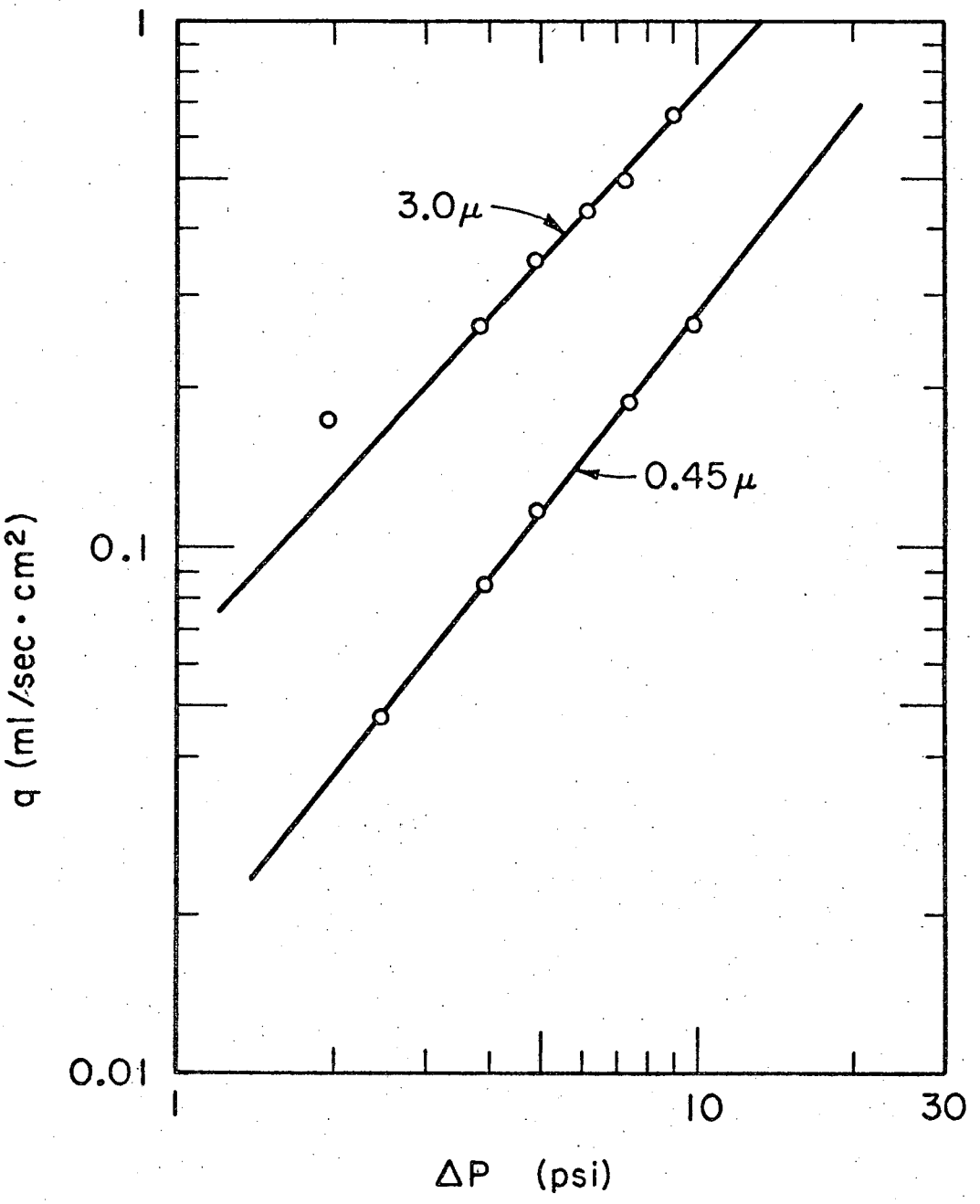

MUB-10680

Fig. 24. Filtration rate/area vs ΔP for clean water at 21°C using Millipore filter membranes. Mean pore diam = 3.0 μ and 0.45 μ.

end, the cake was dried and weighed. From these data the slurry concentration and weight of dry cake per unit area w were obtained. The data are given in Table X and are plotted in Figs. 25 and 26.

Table X. Data for the additivity of cake resistance.

System 1 (1.3 μ slurry)		System 2 (6-14 μ slurry)	
w (mg/cm^2)	R (g_f sec/ml)	w (mg/cm^2)	R (g_f sec/ml)
0.89	5800	0.00	968
1.78	8100	1.76	1050
2.67	10750	3.52	1350
3.56	13150	5.28	1550
4.45	15800	7.05	1790
5.34	18500	8.80	2120
$R = 3000 + 2.86 \times 10^6 w$		$R = 880 + 1.34 \times 10^5 w$	

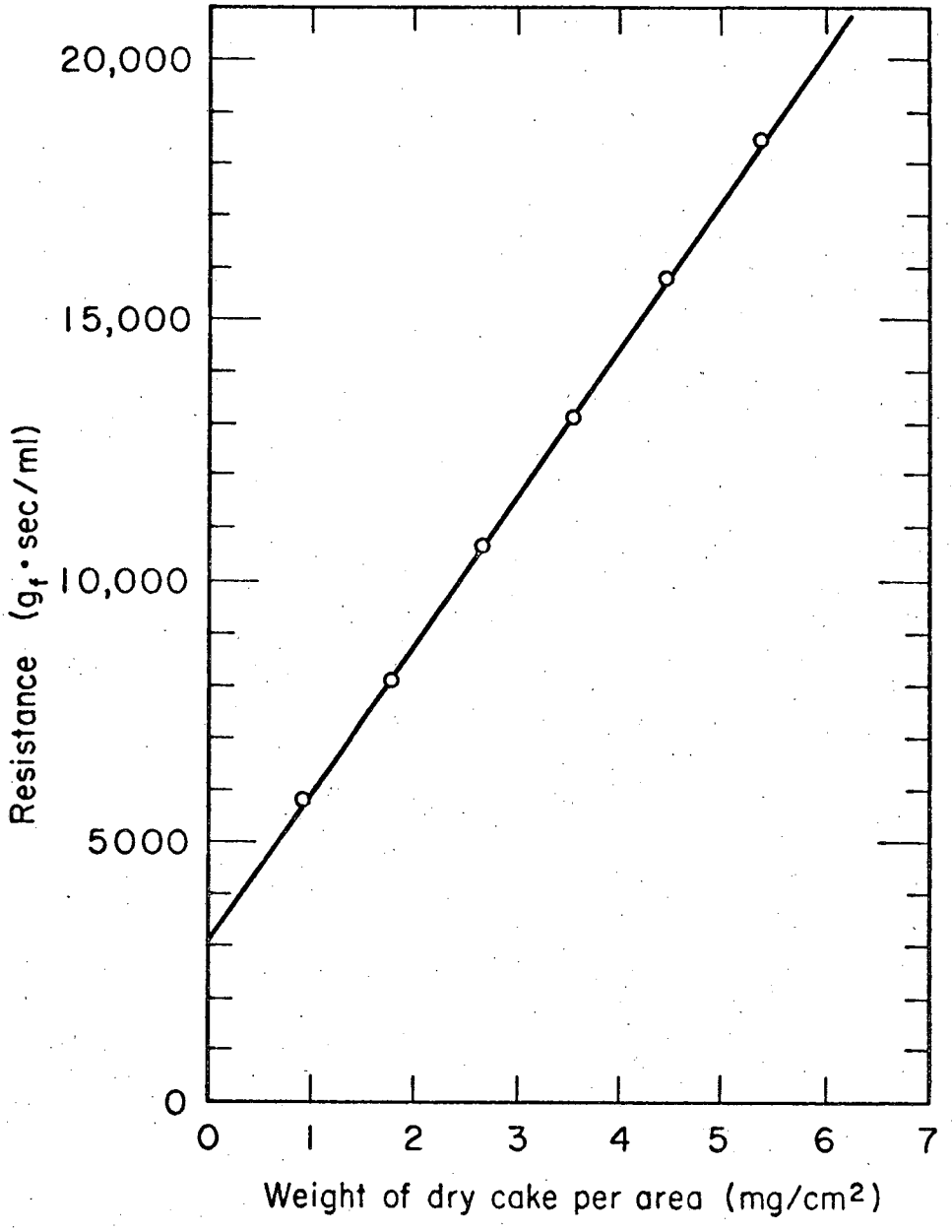

MUB-10675

Fig. 25. Additivity of cake resistance for 1.3 μ slurry confirming Eq. (18).

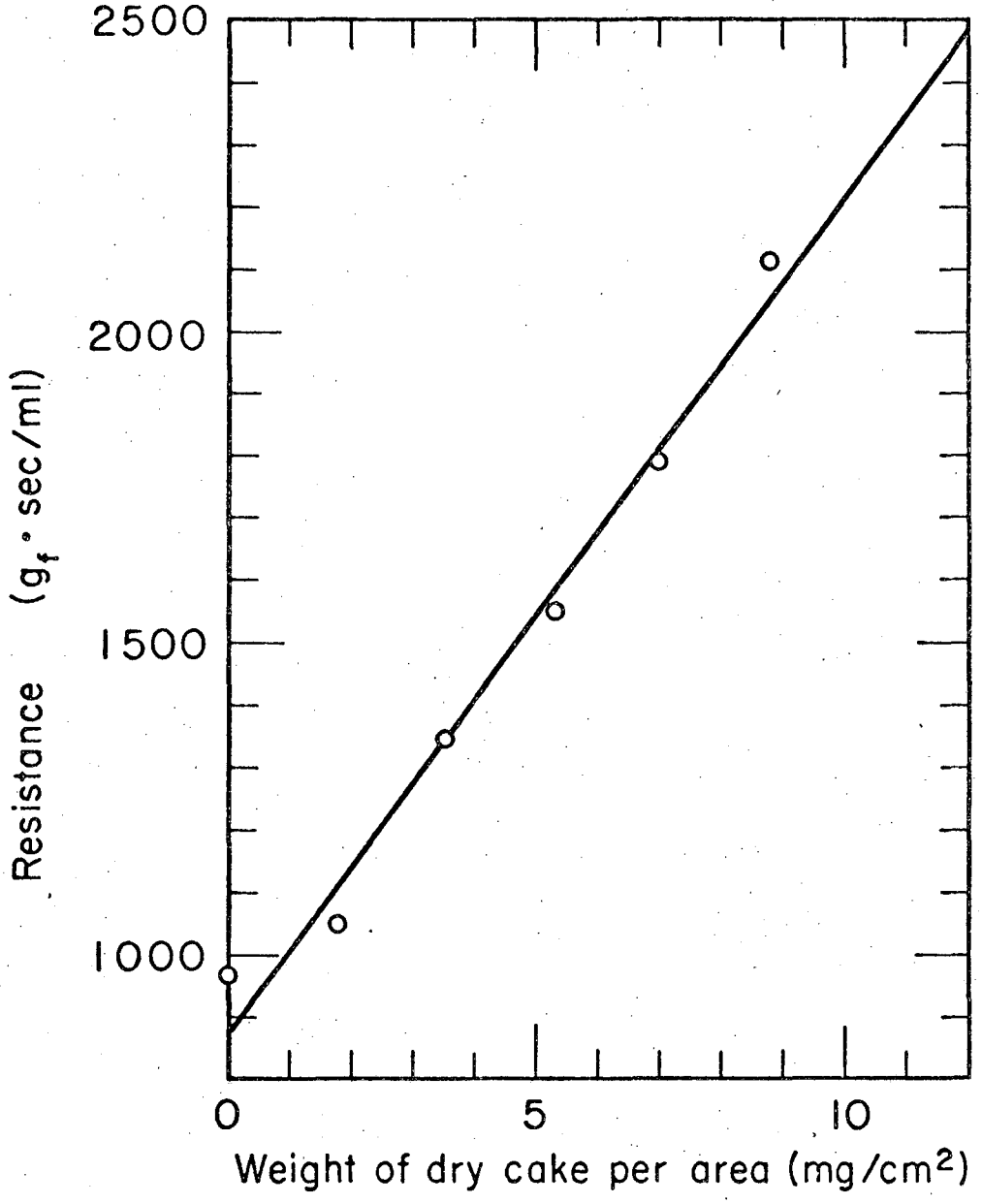

Fig. 26. Additivity of cake resistance for 6 - 14 μ particles confirming Eq. (18).

5. α and β Determination

The slurry was filtered through the membrane and filtrate volume V vs time θ recorded. The data are given in Tables XI and XII and plotted in Figs. 27, 28, 29, and 30. Equation (3) can be rearranged to give

$$\frac{d\theta}{dV} = K_p V + B \tag{83}$$

where

$$K_p = \frac{c\alpha\mu}{A^2 \Delta P\, g_c} \tag{84}$$

$$\beta = \frac{R_m \mu}{A \Delta P\, g_c} \tag{85}$$

c = slurry concentration (g/ml)

From the V vs θ plots $\frac{d\theta}{dV}$ vs V was plotted. The slope K_p of this line gave α and the intercept B gave R_m. R_o and β were calculated using Eqs.(21)and (22).

All the results are summarized in Table XIII.

Table XI. Data for determining α for 1.3 μ slurry at 21°C
$c = 9.5 \times 10^{-4}$ g/ml; $A = 11.35$ cm^2; $\Delta P = 9.55$ psi.

Time (sec)	Filtrate volume (ml)	Data from Fig. 27	
		$\frac{d\theta}{dV}$ (sec/ml)	Filtrate volume (ml)
75	66	0.64	0
120	88	1.51	50
185	112	2.77	100
252	132	4.40	150
308	148	5.22	200
375	162	6.25	250
510	192	7.75	300
645	219	9.70	350
890	260	10.00	400
1035	290	11.40	450
1380	326		
1672	352		
1895	382		
2020	398		
2280	423		
3180	500		

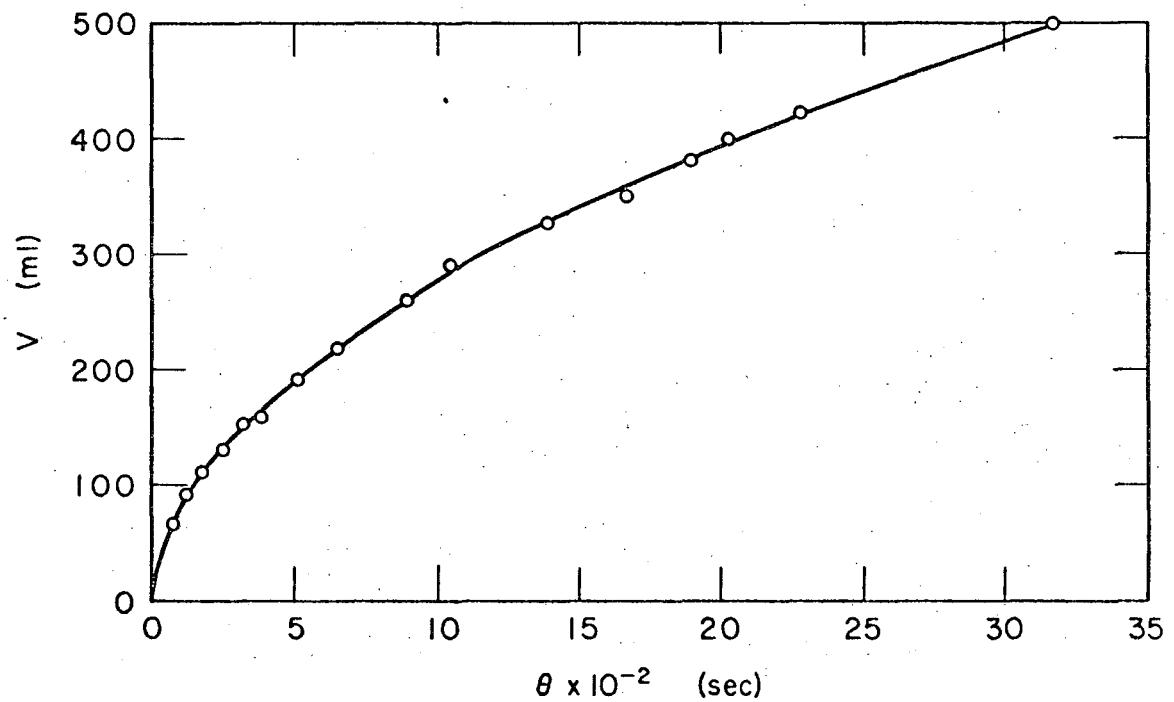

Fig. 27. Filtrate volume vs time for 1.3 μ slurry.

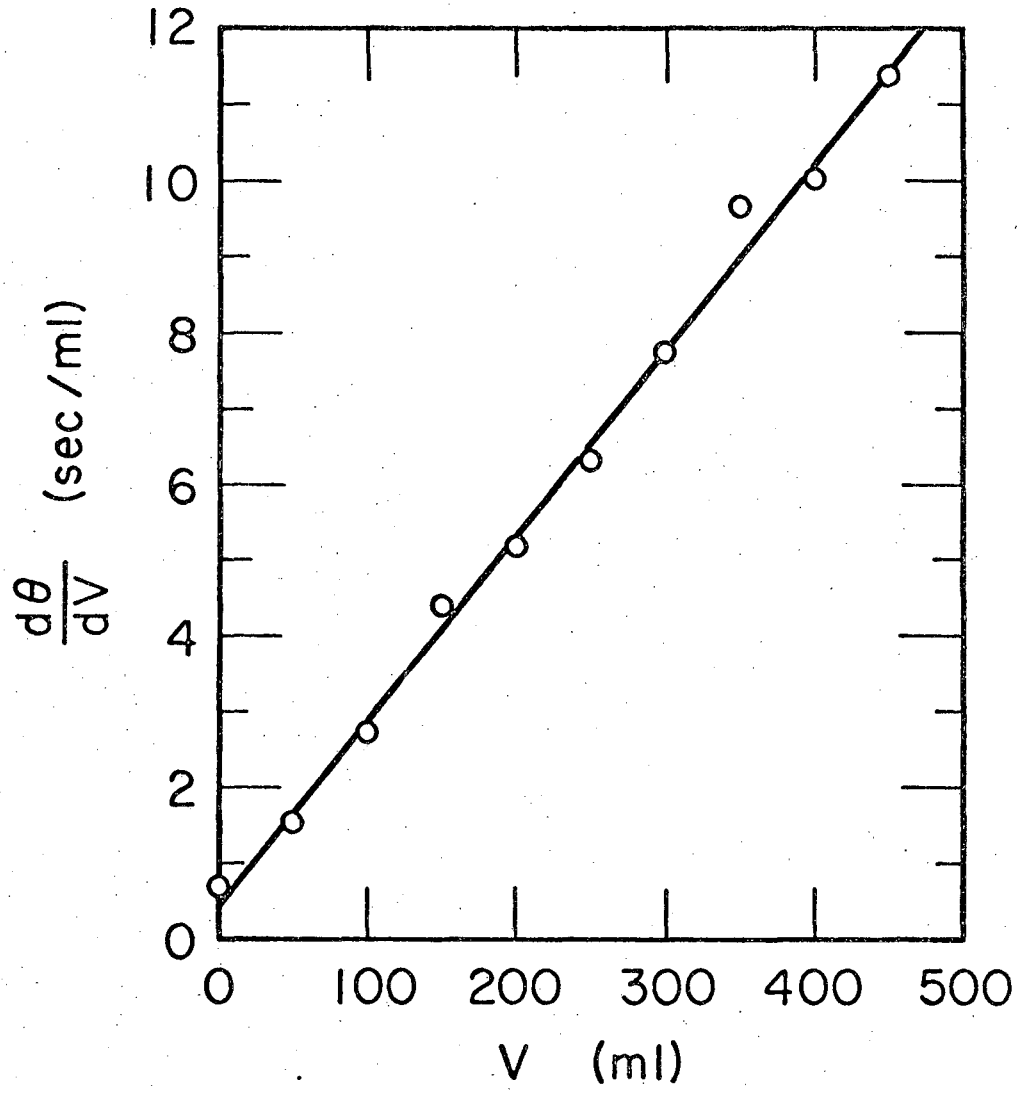

MUB-10679

Fig. 28. $\frac{d\theta}{dV}$ vs V for 1.3 μ slurry. Data from Fig. 27.

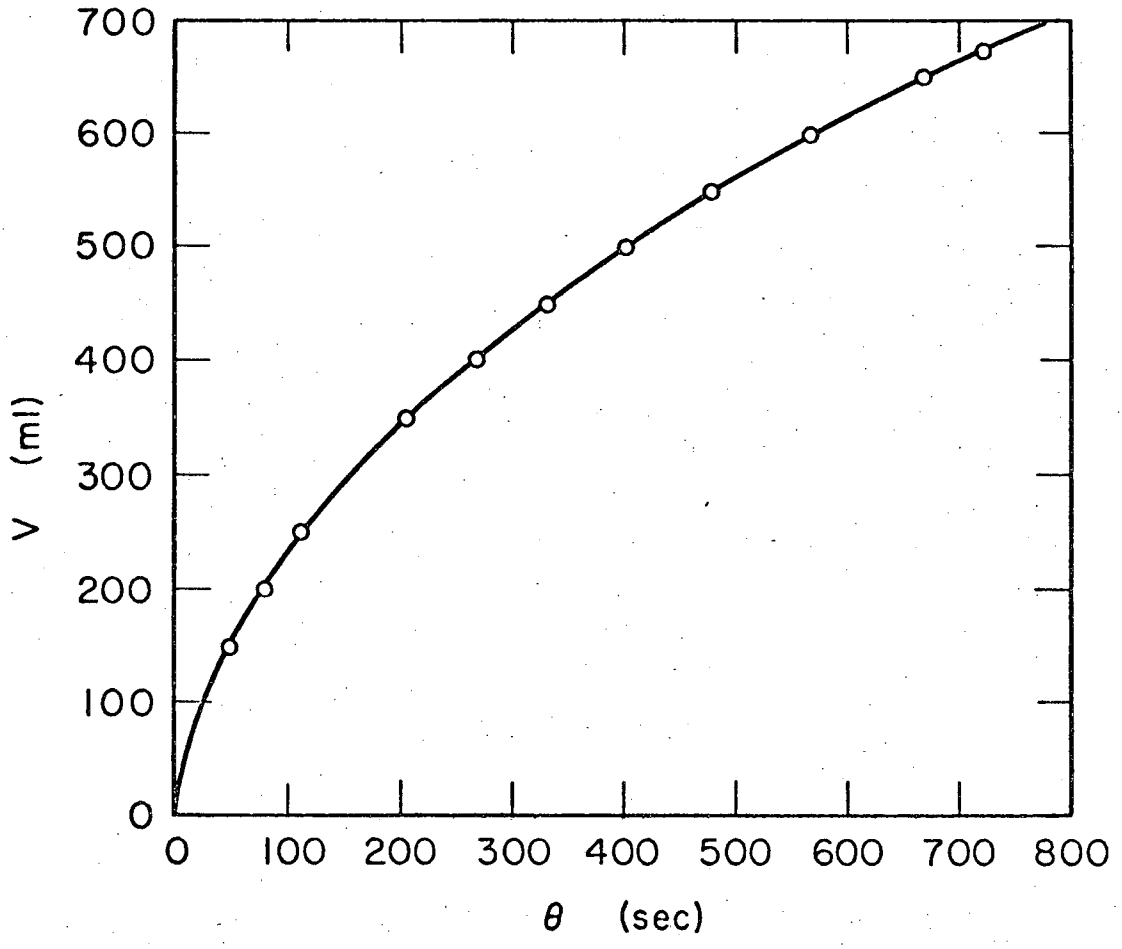

Fig. 29. Filtrate volume vs time for 6 -14 μ slurry.

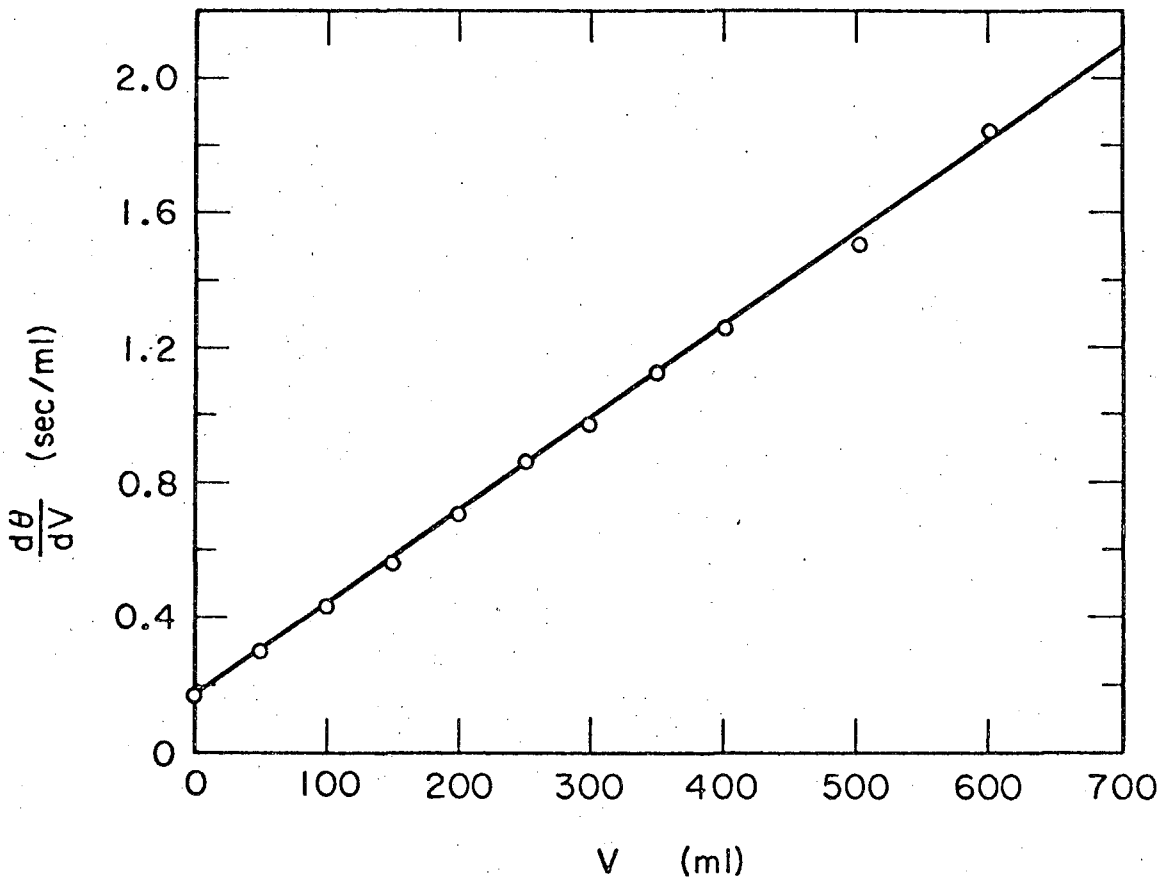

Fig. 30. $\frac{d\theta}{dV}$ vs V for 6 - 14 μ slurry. Data from Fig. 29.

Table XII. Data for determining α for 6 - 14 μ slurry at 21°C. $c = 10.0 \times 10^{-4}$ g/ml; $A = 11.35$ cm^2; $\Delta P = 8.6$ psi.

Time (sec)	Filtrate volume (ml)	Data from Fig. 29	
		$\frac{d\theta}{dV}$ (sec/ml)	Filtrate volume (ml)
50	150	0.172	0
80	200	0.306	50
110	250	0.428	100
205	350	0.558	150
265	400	0.710	200
330	450	0.860	250
400	500	0.975	300
475	550	1.120	350
565	600	1.260	400
665	650	1.500	500
720	675	1.850	600

Table XIII. Summary of the results for the two systems.

Property	Units	1.3 μ system	6-14 μ system
α	cm/g	2.2×10^{11}	2.09×10^{10}
β	g_f sec/cm^4		
from Eq.(23)		1.165×10^6	9.55×10^4
from Eq.(24)		1.34×10^6	5.39×10^4
R_m	cm^{-1}	3.0×10^8	1.075×10^8
R_0	g_f sec/ml		
from Eq.(19)		3000	880
from Eq.(22)		3060	1090
β'	$\frac{g_f \text{ sec cm}^2}{\text{ml. g}}$	2.86×10^6	1.34×10^5
ϵ		0.506	0.575
ρ_c	g/ml	0.520	0.448
ρ_p	g/ml	1.056	1.056

D. Experiments with Rotation

Experimental Procedure. A slurry of about 1 g of solids/liter was prepared in the slurry tank. The rotor was removed from the filter chamber and kept on the stand as shown in Fig. 8. A 4 ×19.5 in. piece of membrane was wetted with distilled water and kept for about 10 minutes to allow to swell (about 1.5%). The wet membrane was wrapped around the rotor and the closing edges were glued together with Millipore cement. A dilute solution of the cement in acetone on slightly wet membrane gave a good joint. Upper and lower edges of the membrane were pressed under the "O" rings and the cover plates and the screws were tightened to secure the filter membrane to the metal screen tightly. Leaks were tested by applying a little air pressure inside the rotor. The rotor assembly was then placed in the filter chamber and the cover flange was secured to the filter chamber by bolts. The slurry in the slurry tank was then pressurized by the nitrogen cylinder to a suitable pressure. The slurry inlet valve was slowly opened to fill the filter chamber, rotor and the filtrate chamber taking care to remove air bubbles. The motor was started and pressure was adjusted to the desired value. During starting of the motor care must be taken to ensure a positive pressure drop across the membrane at all times. This prevents the rupture of the membrane.

It was found that for N greater than 1000 rpm the membrane could not stand the shear. However a cover of nylon cloth improved this strength allowing operation up to 1800 rpm. The nylon cloth cover did not in any way effect the filtration.

1. Limiting Filtration Rate for the 1.3 micron Slurry

The experimental data for the 1.3 micron slurry are given in Table XIV. In the experiments at 800, 1000, and 1200 rpm, total pressure P was kept constant during a run. As Q decreases with time, ΔP_{cl} and ΔP_{ll} also decrease with time and therefore ΔP increases (refer to Eq. (70)). However when the limiting filtration rate Q_∞

has been reached, ΔP_{cl}, ΔP_{ll} and ΔP all become constant. The data for these runs at 800, 1000, and 1200 rpm are plotted in Figs. 31, 32 and 33. The experimental data for runs at 1400 and 1800 rpm are given in Table XVI. Figure 34 shows the data for the run at 1800 rpm. In this run at 1800 rpm, P was so adjusted to give constant ΔP. In this run ΔP = 4, 8, 12, 16 and 24 psi was applied to see if Q_∞ had any dependence on ΔP.

Comparison of the Experimental and the Calculated Values of q_∞ The experimental data for the 1.3 micron slurry are summarized in Table XVI and compared with the values predicted by the simple centrifugal force model (Eq. (36)) and the improved particle diffusion model (Eq. (59)). In calculating u from Eq. (36) it was assumed that the tangential velocity of the particle is the same as that of the membrane. Viscosity of pure water at 25°C was used. D_p is taken as the diameter of the smallest particle in the slurry. For the particle diffusion model u_{to} was estimated by Eq. (36) assuming that a particle aquires its terminal velocity instantaneously at all points. τ_w was obtained from the P_τ data of Fig. 2., using Eqs. (80) and (81). The boundary layer thickness, δ was computed from Eqs. (30) and (54). Molecular diffusivity of particles, D was computed from Eq. (48) and ϵ_o was computed from Eq. (47) using τ_w as obtained from Eq. (81). From Eq. (61) u_d was calculated using $c_w = 0.509$ and $c_b = 0.95 \times 10^{-3}$. It was assumed that c_w is equal to the weight fraction of solids in the bulk of the wet cake. c_w can be easily calculated from the porosity data of the cake as determined in filtration experiments without rotation. Total u was obtained as the sum of u_{to} and u_d. A sample calculation is shown in Appendix B.

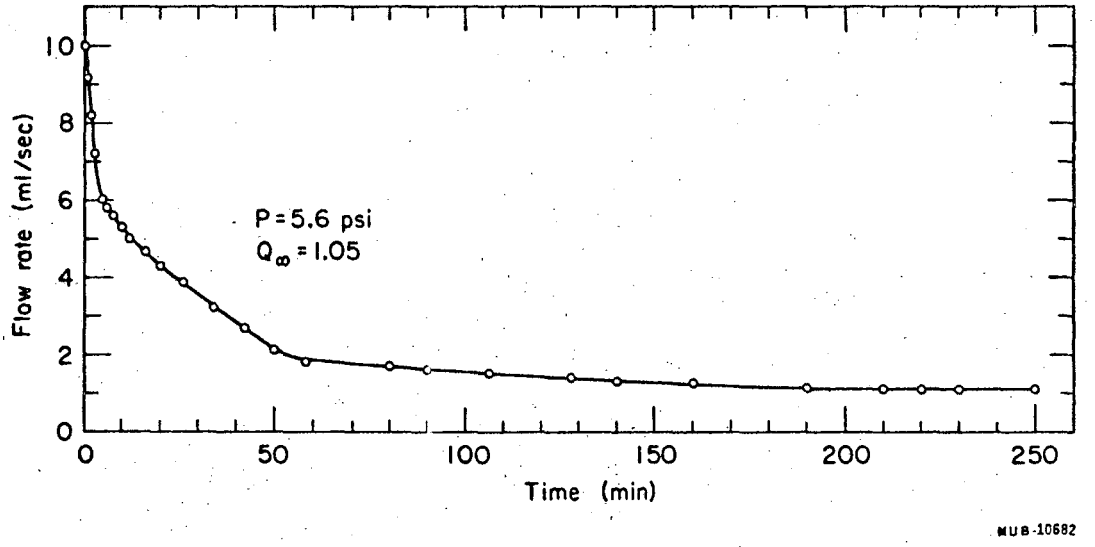

Fig. 31. Filtration rate vs time for 1.3 μ slurry at 25°C and 800 rpm.

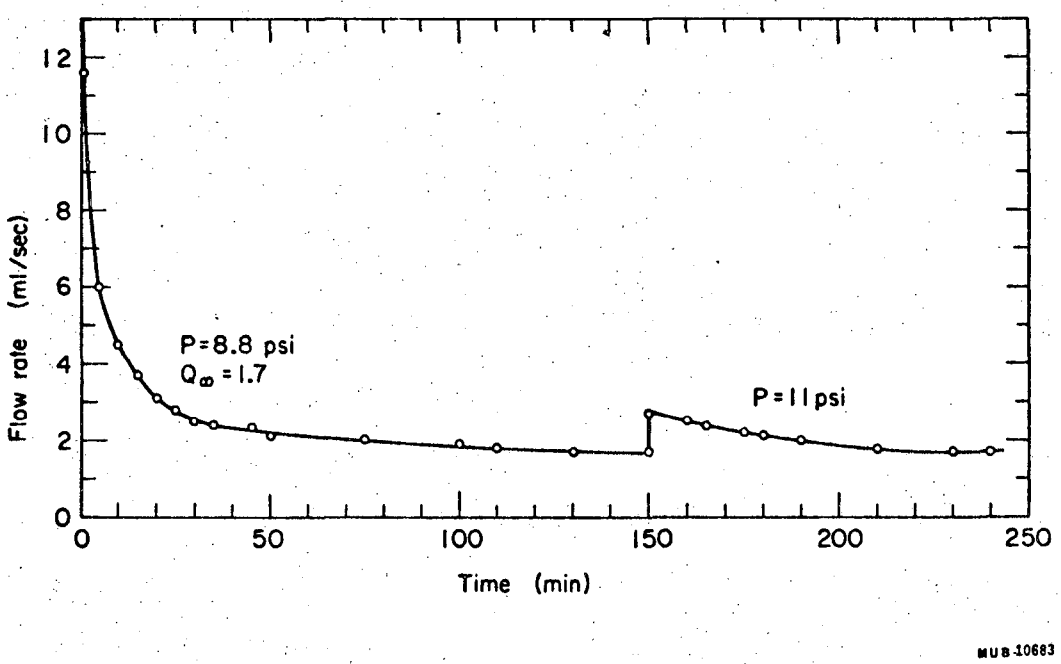

Fig. 32. Filtration rate vs time for 1.3 μ slurry at 25°C and 1000 rpm.

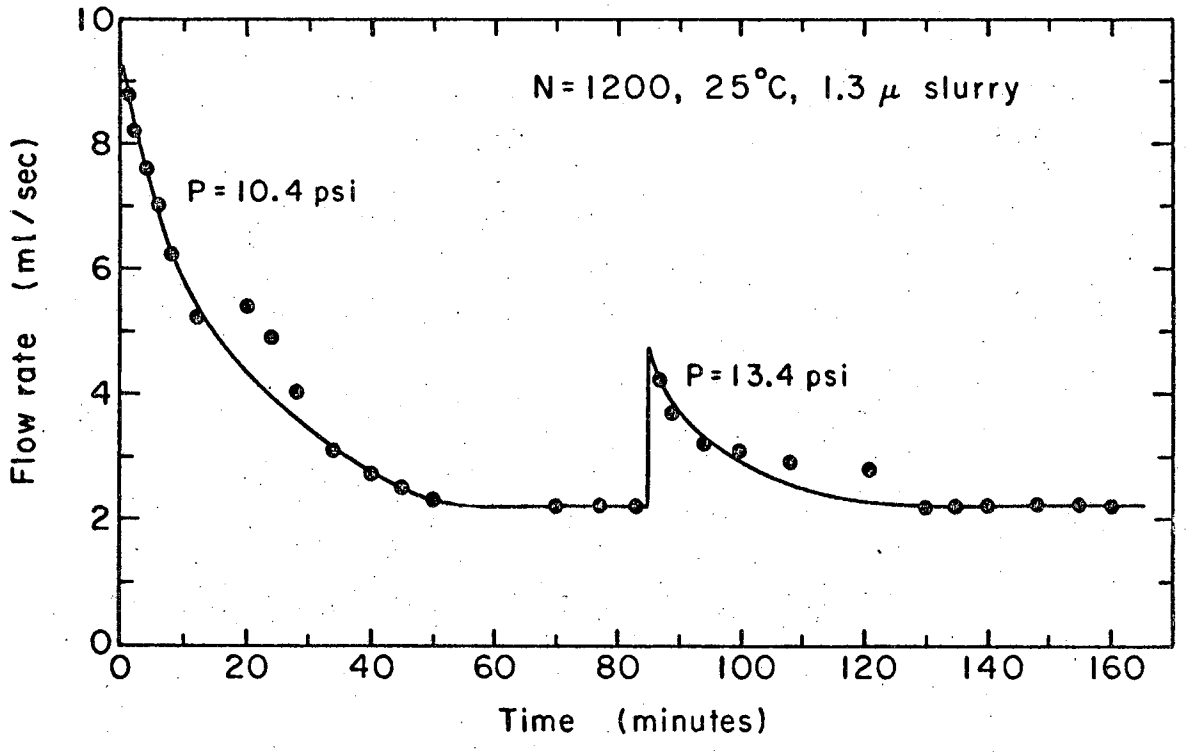

VARIATION OF FILTRATION RATE WITH TIME

MUB-9711

Fig. 33. Filtration rate vs time for 1.3 μ slurry at 25°C and 1200 rpm.

Table XIV. Experimental data for limiting filtration rate for 1.3 μ slurry at 25°C. A = 364 cm^2.

Run no. 110 N = 800 rpm		Run no. 120 N = 1000 rpm		Run no. 130 N = 1200 rpm	
Time (min)	Flow rate (ml/sec)	Time (min)	Flow rate (ml/sec)	Time (min)	Flow rate (ml/sec)
P = 5.6 psi		P = 8.8 psi		P = 10.4 psi	
0	10.0	1	11.6	1	8.8
1	9.2	5	6.0	2	8.2
2	8.2	10	4.5	4	7.4
3	7.2	15	3.7	6	7.0
5	6.0	20	3.1	8	6.2
6	5.8	25	2.8	12	5.2[b]
8	5.6	30	2.5	20	5.4
10	5.3	35	2.4	24	4.9
12	5.0	45	2.3	28	4.0
16	4.7	50	2.1	34	3.1
20	4.3	75	2.0	40	2.7
26	3.9	100	1.9	45	2.5
34	3.2	110	1.8	50	2.3
42	2.7	130	1.7	70	2.2
50	2.1	150	1.7	77	2.2
58	1.87	P = 11.0 psi		83	2.2
66	1.80	150	2.7	P = 13.4 psi[a]	
80	1.67	160	2.5	87	4.2
90	1.60	165	2.4	89	3.7

Table XIV (Continued)

N = 800 rpm		N = 1000 rpm		N = 1200 rpm	
Time (min)	Flow rate (ml/sec)	Time (min)	Flow rate (ml/sec)	Time (min)	Flow rate (ml/sec)
106	1.53	175	2.2	94	3.2
128	1.43	180	2.1	100	3.1
140	1.36	190	2.0	108	2.9
190	1.13	210	1.75	121	2.8
210	1.05	230	1.70	130	2.2
220	1.05	240	1.70	135	2.2
250	1.05			140	2.2
				148	2.2
				155	2.2
				160	2.2

[a] initially P was little higher

[b] there were some air bubbles in the rotameter

Table XV. Experimental data for limiting filtration rate for 1.3 μ slurry at 25°C. A = 364 cm^2.

Run No. 140
N = 1400 rpm

Time (min)	Flow rate (ml/sec)	Time (min)	Flow rate (ml/sec)
ΔP = 4.0 psi		ΔP = 8.0 psi	
1	18.4	42	7.4
2	14.6	45	5.6
3	12.2	49	5.0
4	10.8	55	4.5
6	10.0	60	4.2
8	8.0	65	4.0
10	6.6	70	3.9
12	6.0	75	3.7
14	5.2	80	3.6
16	5.0	85	3.6
18	4.8	90	3.4
20	4.4	95	3.4
24	4.0	100	3.4
28	3.6		
32	3.4		
36	3.4		
41	3.4		

Table XV. (Continued)

Run no. 150
N = 1800 rpm

Time (min)	Flow rate (ml/sec)	Time (min)	Flow rate (ml/sec)
ΔP = 4.0 psi		ΔP = 16 psi	
4	15.0	48	7.8
5	13.4	49	7.0
7	11.6	50	6.6
8	9.6	51	6.0
9	8.6	53	5.8
10	8.6	58	5.2
11	8.0	60	5.2
14	7.4	ΔP = 24 psi	
16	7.4	61	8.2
ΔP = 8.0 psi		62	7.8
16	14.6	63	7.2
18	13.4	64	7.0
19	11.6	65	6.6
20	10.8	66	6.4
21	10.2	67	6.0
22	9.0	68	6.0
24	8.0	69	5.8
28	6.6	70	5.6
30	6.6	73	5.6
ΔP = 12.0 psi		75	5.4
31	9.6		
32	8.2		
33	7.4		
34	7.2		
35	7.0		
36	6.6		
40	6.0		
47	5.2		

Table XVI. Summary of the experimental data on q_∞ for the 1.3 μ slurry.

Run no.	N (rpm)	Z_0	Q_{∞} expr. $\frac{ml}{sec}$	q_{∞} expr. $\frac{ml}{sec\ cm^2} \times 10^3$	τ_w $\frac{g_f}{cm^2}$	a (cm^{-1})	δ (μ)	ϵ_0 $\frac{cm^{-1}}{sec}$	A (μ)	u_{t0} $\frac{cm}{sec} \times 10^4$	u_d $\frac{cm}{sec} \times 10^3$	u_{calc} $\frac{cm}{sec} \times 10^3$
110	800	54.3	1.05	2.88	0.521	89	56	0.592	0.865	3.07	2.29	2.60
120	1000	84.8	1.70	4.66	0.988	136	36.8	1.57	0.628	4.78	3.20	3.68
130	2000	122.0	2.20	6.04	1.68	193	25.9	3.48	0.481	6.90	4.16	4.85
140	1400	166.0	3.40	9.33	2.66	258	19.4	6.80	0.385	9.35	5.21	6.15
150	1800	275.0	5.20	14.20	5.68	415	12.0	21.1	0.265	15.55	7.65	9.21

$D_p = 1.3\ \mu$; $C_b = 0.95 \times 10^{-3}$; $C_w = 0.509$

2. Limiting Filtration Rate for the 6 - 14 micron Slurry

The experimental data for the 6 - 14 μ slurry (conc. = 0.768 g/l) at 25°C are given in Table XVII. All these experiments were done with the same membrane. The experiment was started at N = 1000 rpm and at the end of the run the rpm was changed to 800 and then to 600. Total pressure P was kept constant during a run. These data are plotted in Figs. 35, 36 and 37. Table XVIII gives data for N = 1400 and N = 0. This clearly shows the effect of rotation on filtration. For the run at 1400 rpm, distilled water was continuously fed to the slurry tank and the filtrate was rejected. The solids accumulated in the filter chamber (conc. = 3.66 g/l). Figure 38 shows the data for the runs at N = 1400 and N = 0.

Another series of experiments were performed (run nos. 231 and 232) with 6 - 14 μ slurry containing varying amounts of sodium chloride, to see the effect of liquid density on q_∞. The data for these runs are given in Table XIX. and plotted in Fig. 39. The experimental data for the 6 - 14 μ slurry are summarized in Table XX. and compared with the values predicted by the simple centrifugal force model Eq. (36) and the improved particle diffusion model Eq. (59). All the terms u_{t0}, τ_w, a, δ, ϵ_0, D, A and u_d were calculated as explained for the 1.3 μ slurry. D_p = 6.0 was used in these calculations. It was assumed that c_w is the weight fraction of solids in the bulk of the wet cake and was equal to 0.466. c_b was taken to approximately 2.0×10^{-3}.

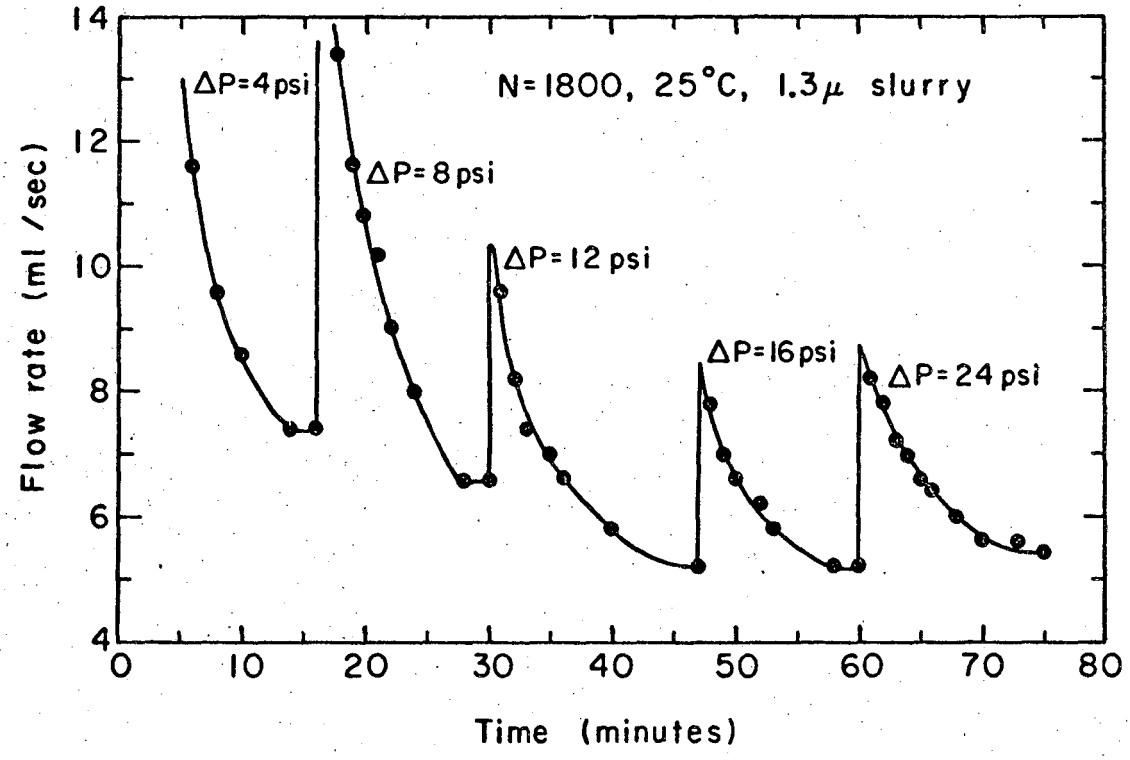

MUB-9712

Fig. 34. Filtration rate vs time for 1.3 μ slurry at 25°C and 1800 rpm.

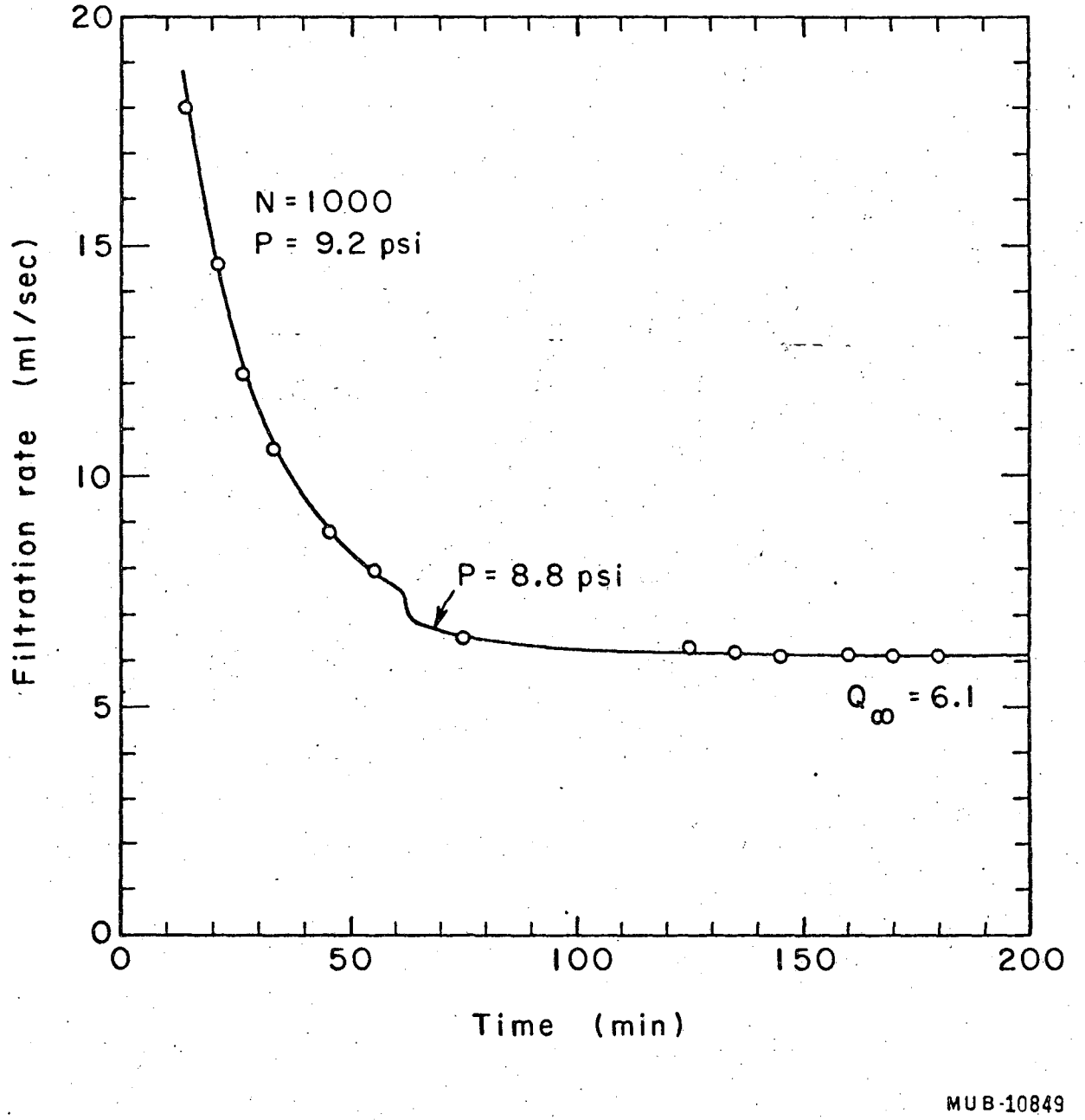

Fig. 35. Filtration rate vs time for 6 - 14 μ slurry at 25°C and 1000 rpm.

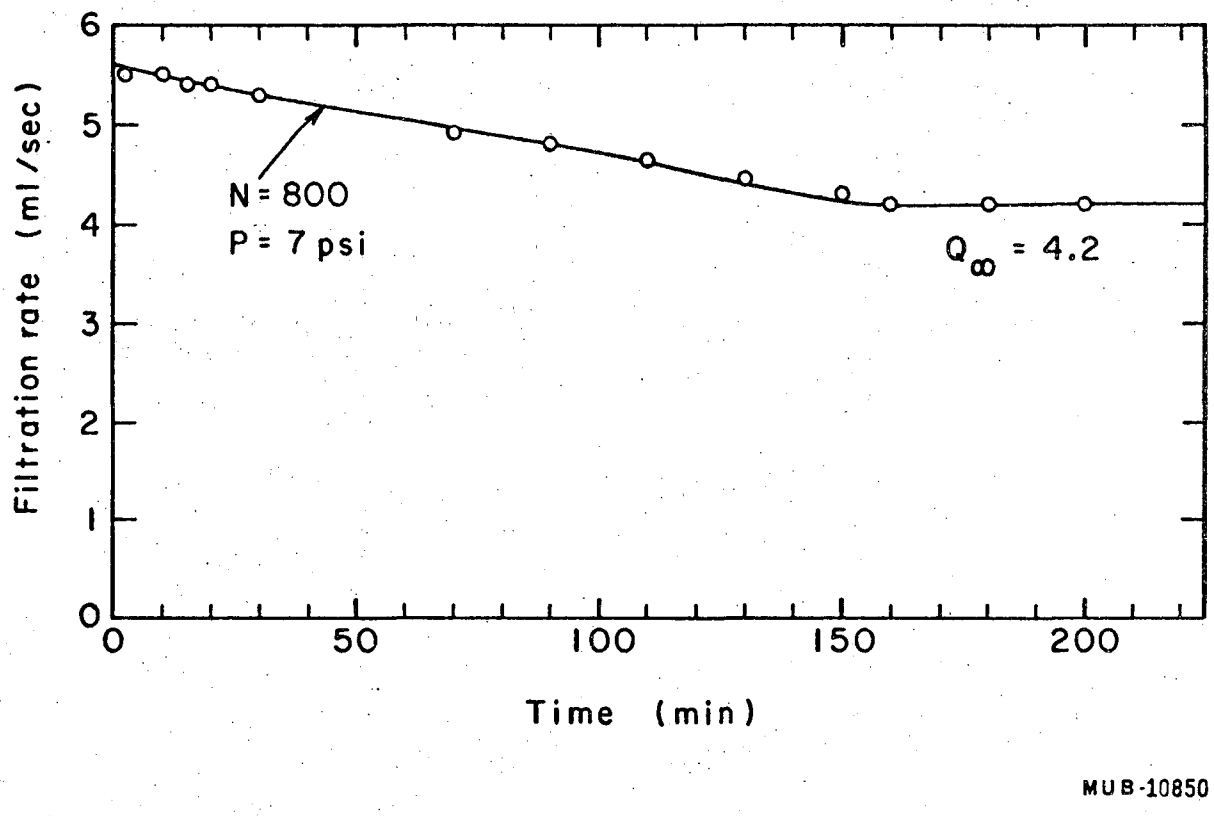

Fig. 36. Filtration rate vs time for 6 - 14 μ slurry at 25°C and 800 rpm.

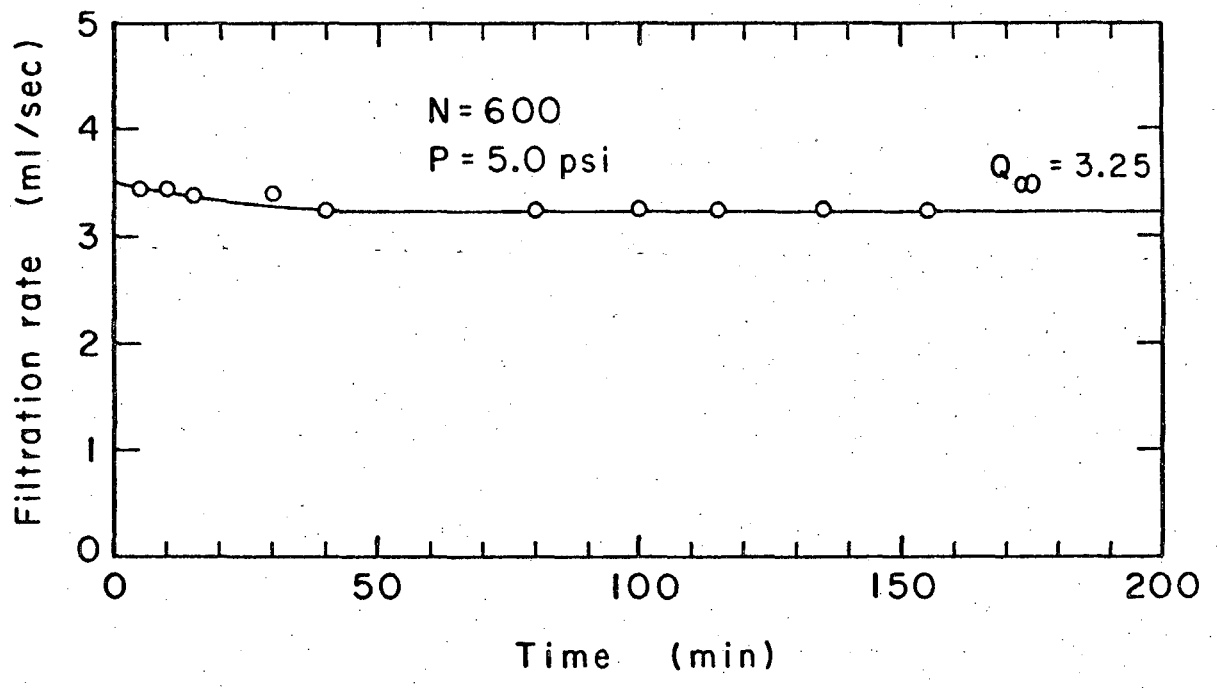

Fig. 37. Filtration rate vs time for 6 - 14 μ slurry at 25°C and 800 rpm.

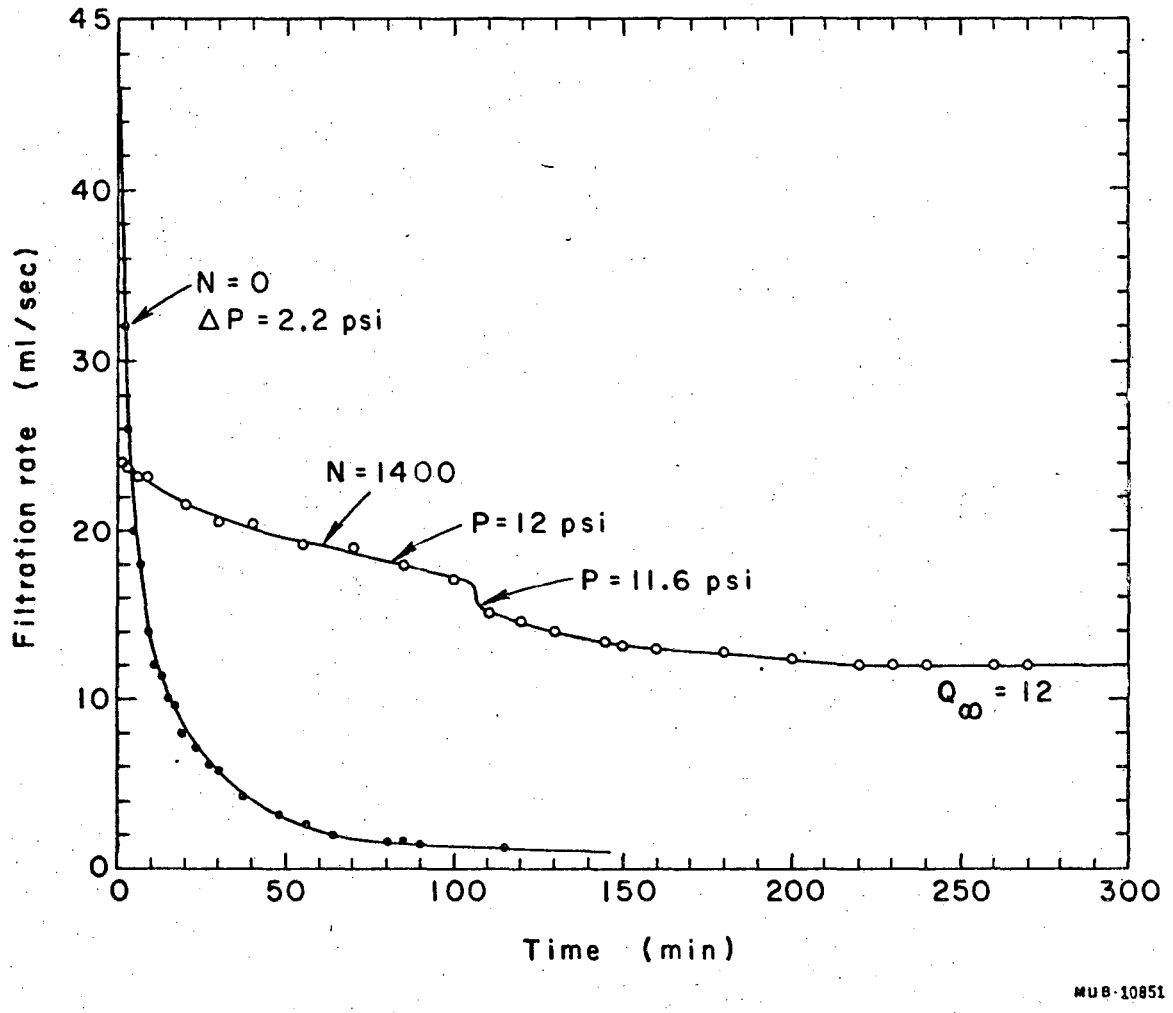

Fig. 38. Filtration rate vs time for 6 - 14 μ slurry at 25°C and 1400 rpm and no rotation. Results clearly show the effect of rotation on the filtration rate and total throughput.

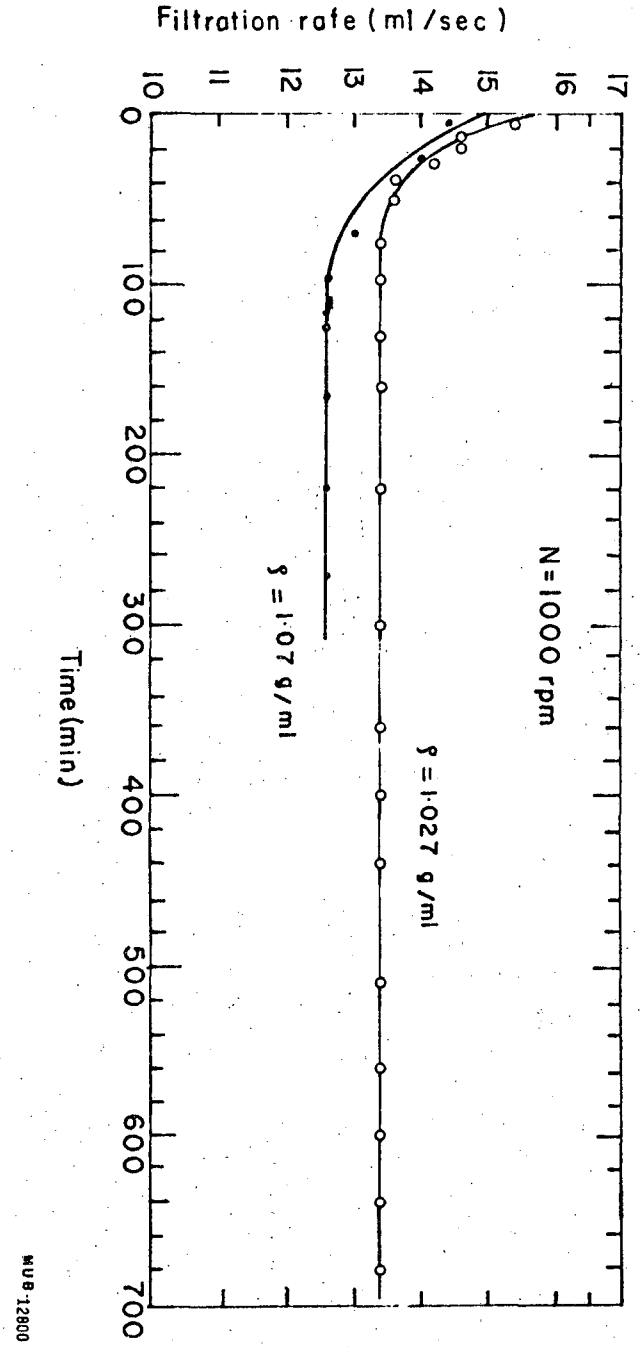

Fig. 39. Filtration rate vs time for 6 - 14 μ slurry at 25°C and 1000 rpm containing sodium chloride.

Table XVII. Experimental data for the limiting filtration rate for the 6 - 14 μ slurry at 25 C. A = 364 cm^2.

Run no. 230 N = 1000		Run no. 220 N = 800		Run no. 210 N = 600	
Time (min)	Flow rate (ml/sec)	Time (min)	Flow rate (ml/sec)	Time (min)	Flow rate (ml/sec)
P = 9.2 psi		P = 7.0 psi		P = 5.0 psi	
0	42.0	2	5.5	5	3.45
2	37.0	10	5.5	10	3.45
5	32.8	15	5.4	15	3.40
10	24.4	20	5.4	30	3.40
14	18.0	30	5.3	40	3.25
21	14.6	70	4.9	80	3.25
26	12.2	90	4.8	100	3.25
33	10.6	110	4.65	115	3.25
45	8.8	130	4.45	135	3.25
55	8.0	150	4.30	155	3.25
P = 8.8 psi		160	4.20		
75	6.5	180	4.20		
125	6.3	200	4.20		
135	6.2				
145	6.1				
160	6.1				
170	6.1				
180	6.1				

Table XVIII. Experimental data for the limiting filtration rate for the 6 - 14 μ slurry at 25°C. A = 364 cm^2.

Run no. 250 N = 0		Run no. 240 N = 1400 rpm			
Time (min)	Flow rate (ml/sec)	Time (min)	Flow rate (ml/sec)	Time	Flow rate
P = 2.2 psi		P = 12.0 psi		P = 11.6 psi	
0	54.0	1	24.0	110	15.2
1	40.0	3	23.8	120	14.6
2	32.0	6	23.2	130	14.0
3	26.0	9	23.2	145	13.4
5	20.0	20	21.6	150	13.2
7	18.0	30	20.6	160	13.0
9	14.0	40	20.4	180	12.8
11	12.0	55	19.2	200	12.4
13	11.4	70	19.0	220	12.0
15	10.0	90	18.0	230	12.0
17	9.6	100	17.2	240	12.0
19	8.0			260	12.0
23	7.2			270	12.0
27	6.2				
30	5.8				
37	4.2				
48	3.2				
56	2.7				
64	2.0				
80	1.7				
85	1.6				
90	1.5				
115	1.3				

Table XIX. Experimental data for limiting filtration rate for 6-14 slurry containing sodium chloride at 25°C.

N = 1000 and A = 364 cm^2			
Run no. 231		Run no. 232	
4.05% sodium chloride solution ρ= 1.027 g/ml; μ = 0.987 cp		9.8% sodium chloride solution ρ = 1.08 g/ml; μ = 1.08 cp	
Time (min)		Time (min)	
P = 6.2 psi		P = 6.4 psi	
7	15.4	0	14.4
12	14.6	5	14.4
19	14.6	15	14.4
27	14.2	25	14.0
37	13.6	40	13.6
55	13.6	55	13.6
75	13.4	70	13.0
95	13.4	95	12.6
130	13.4	125	12.6
160	13.4	165	12.6
220	13.4	220	12.6
300	13.4	270	12.6
360	13.4		
400	13.4		
440	13.4		
510	13.4		
560	13.4		
600	13.4		
640	13.4		
680	13.4		

Table XX. Summary of the experimental data on q_∞ for 6-14 μ slurry.

Run no.	N (rpm)	Z_0	Q_∞ expr. $\frac{ml}{sec}$	$q_\infty \times 10^3$ expr. $\frac{ml}{sec\ cm^2}$	τ_w $\frac{g_f}{cm^2}$	a (cm^{-1})	δ (μ)	ϵ_0 $\frac{cm^{-1}}{sec}$	A (μ)	$u_{t0} \times 10^3$ $\frac{cm}{sec}$	$u_d \times 10^3$ $\frac{cm}{sec}$	$u_{calc} \times 10^3$ $\frac{cm}{sec}$
210	600	30.6	3.25	8.94	0.225	51.6	97	0.169	0.783	3.96	0.465	4.4
220	800	54.3	4.20	11.55	0.521	89.0	56	0.592	0.515	7.05	0.706	7.76
230	1000	84.8	6.10	16.75	0.988	136.0	36.8	1.570	0.376	11.10	0.996	12.10
240	1400	166.0	12.0	33.0	2.660	258.0	19.4	6.80	0.228	21.70	1.590	23.30

VI. DISCUSSION OF RESULTS AND CONCLUSIONS

A. Resistance Concept

The resistance concept as developed in Sec. III-B has been found to be very useful in analysis of filtration data for constant pressure filtration—especially the case when neither the pressure drop across the membrane ΔP nor the filtration rate Q is constant. Dependence of the cake resistance R on the cake thickness L as given by Eqs (17) and (18) is very well followed by the two systems of slurries as clearly shown by Figs. 25 and 26. The thickness coefficient of cake resistance β is larger for smaller particles as they make a more compact cake and offer higher resistance to flow. This concept has been further used to estimate the cake thickness L applying Eq. (74).

B. Fluid Drag

The experimental data on fluid drag on rotating cylinders was correlated in terms of a drag coefficient C_D and a Reynolds number Re_D, as done previously by Theodorsen and Regier.[18] Reynolds' number was based on rotor diameter as suggested by Eisenberg, Tobias, and Wilke.[9] During mass transfer studies with rotating cylinders these authors found that for turbulent flow, a Reynolds number based on rotor diameter characterized the system satisfactorily. Theodorsen and Regier[18] have also defined their Reynolds number based on rotor diameter, rather than the gap width. Drag coefficients computed from the data of this study do not agree with the data of Theodorsen and Regier[18] with respect to the Reynolds number dependence. Both results are compared in Fig. 22. Our data indicate that the drag coefficient C_D is proportional to $Re_D^{0.9}$ (for $6 \times 10^5 < Re_D < 17 \times 10^5$) whereas their work indicates that C_D is proportional to $Re_D^{-0.3}$ (for $10^4 < Re_D < 6 \times 10^5$). Our drag coefficients have the same general magnitude and are approximately equal to Theodorsen and Regier's results at $Re_D \simeq 6 \times 10^5$.

C. Limiting Filtration Rate

During the filtration runs with rotating membranes it was found that in each case a constant filtration rate is reached which is quite characteristic of the slurry system and the rpm of the rotor. This value of the limiting filtration rate/area, q_∞ is independent of ΔP of filtration as shown by Figs. 32, 33, and 34. For example in run no. 120 (Fig. 32) filtration starts with Q = 12 ml/sec and reaches a constant value of 1.7 ml/sec after about 130 minutes ($V \simeq 20$ liters). At this point ΔP and Q do not change with time. In other words the cake reaches a thickness which does not increase with time and filtration can be continued indefinitely without any further cake formation. If at this point pressure is increased, the flow rate increases for a time but again falls to the same constant Q_∞ values of 1.7 ml/sec. This clearly shows that the cake resistance (and therefore the cake thickness) has increased but the limiting filtration rate is the same. Thus it can be inferred that for a given particle system and rpm it is the limiting filtration rate which is characteristic and not the cake resistance.

For the run at 1400 rpm using 6-14 μ slurry (Fig. 38) the cake resistance becomes 2,340 g_f sec/ml after giving a throughput of about 280 liters. If the filtration is carried out without rotation (run no. 250), the cake resistance becomes 43,200 g_f sec/ml after giving a throughput of about 37 liters. This comparison clearly shows that the rotation of the membrane prevents cake formation and increases the throughput of a filter membrane many-fold.

Experimental data indicate that q_∞ is proportional to Z_0 or N^2 and q_∞ is larger for larger particles at the same rpm. Predicted values of q_∞ are compared with the experimental values in Fig. 40. It is clear that the simple centrifugal force model fails badly to predict q_∞ for the 1.3 micron particles. The improved model including the effect of particle diffusion predicts q_∞ within 35% for both the 1.3

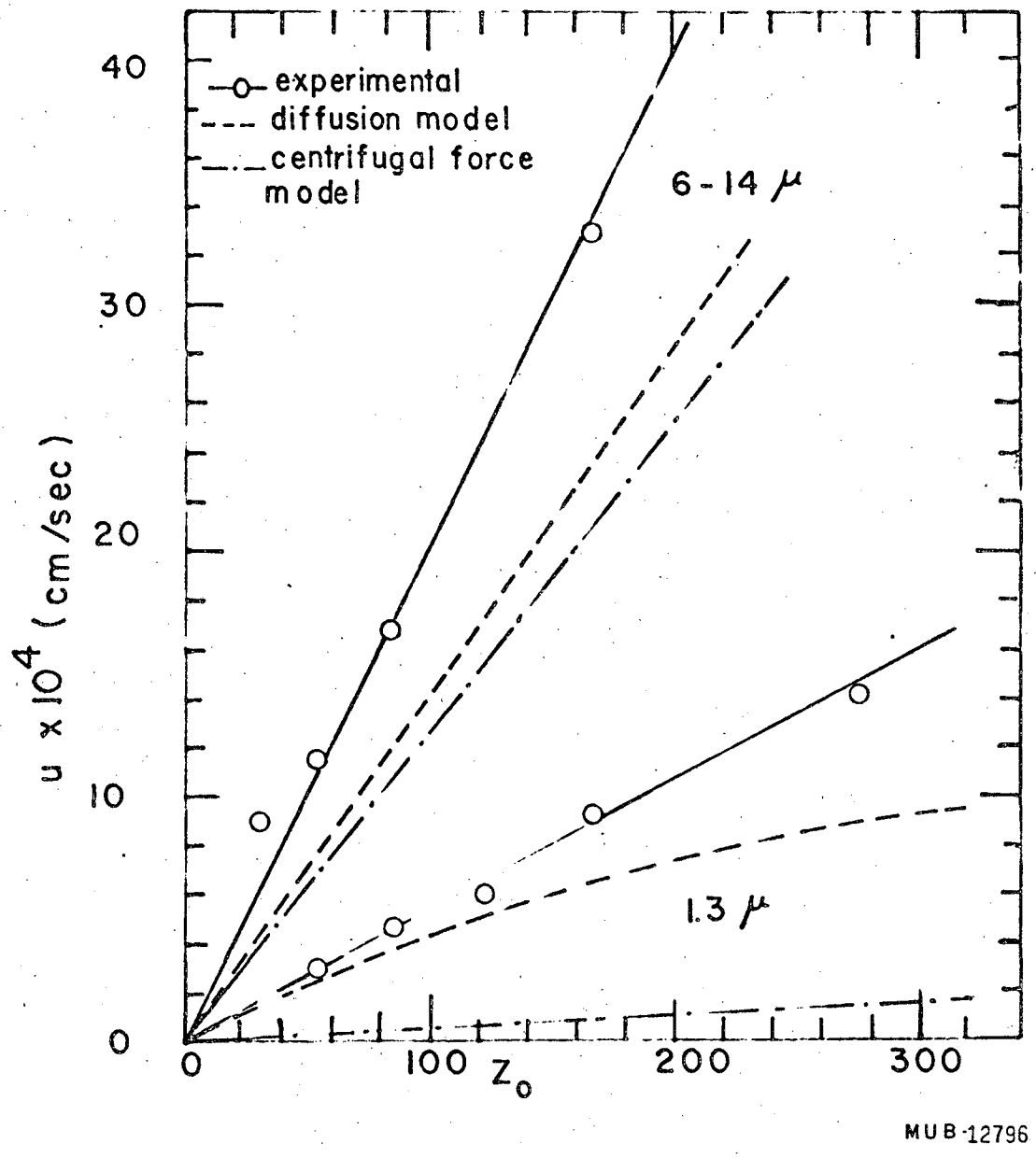

Fig. 40. Comparison of the experimental values of limiting filtration rate/area vs rpm and the predicted values by the two models.

micron and 6-14 μ systems. All the predicted values are lower than the experimental values.

The improved model including the effect of particles diffusion indicates that there are two terms in the expression for u in Eq (60).

$$u = u_{t0} + u_d \tag{60}$$

where u_{t0} is the centrifugal term (Eq. (36)) and u_d is the diffusion term (Eq. (62)).

$$u_d = 0.0613\frac{\sqrt{\tau_w g_c}}{\sqrt{\rho}}\left(\frac{D}{\nu}\right)^{2/3} \ell n\frac{c_w}{c_b} \tag{62}$$

Calculations show that u_d(Eq. (62)) is larger for smaller particles and increases with rpm for a given particle size. Eddy diffusion will be expected to have greater effect on smaller particles because the size of smaller eddies will be comparable to the particle size. From Eqs. (62) and (48), u_d is proportional to $D_p^{-2/3}$. For a given particle size, u_d will be expected to be larger at higher rpm because greater turbulence will cause more diffusion. From Eqs. (62) and (81) it will be seen that u_d is proportional to $N^{1.45}$.

Experiment nos. 231 and 232 show that q_∞ is not proportional to $(\rho_p-\rho)$ as is predicted by the simple centrifugal force model Eq. (36).

$$u_{t0} = \frac{D_p^2(\rho_p-\rho)g}{18\mu} Z_0 \tag{36}$$

In run no. 232 liquid density is greater than that of the particles. If the centrifugal force model was true, we would expect all the particles to be forced to the membrane and the limiting filtration rate/area, q_∞ to be very small (approaching zero) because of the cake formed. Our run no. 232 clearly indicates that q_∞ is constant and of substantial magnitude. This evidence supports the improved model including particle diffusion.

1. Effect of System Properties on the Limiting Filtration Rate/Area

. The limiting filtration rate/area, q_∞ will be effected by system properties like rotor rpm, liquid and particle density, liquid viscosity and particle diameter, etc. These effects are briefly discussed below.

a. Effect of Particle Diameter. Simple centrifugal force model predicts that q_∞ is proportional to D_p^2 (Eq. (36)). However from our data on two particle sizes 1.3 μ and 6 - 14 μ we find that q_∞ is approximately proportional to $D_p^{0.9}$. At a constant rpm from Eq. (62) u_d is proportional to $D_p^{-2/3}$. Thus according to the diffusion model

$$u = k_1 D_p^2 + k_2 D_p^{-2/3} \tag{86}$$

where k_1 and k_2 are two constants. Equation (86) supports the observation that q_∞ is proportional to a power of D_p less than 2, and therefore that the 0.9 power dependence may be reasonable.

b. Effect of rpm of the Rotor. Our experimental data indicate that q_∞ is proportional to N^2 or Z_0. This is exactly what is predicted by the centrifugal force model. However the quantitative agreement of the data with the simple centrifugal force model is very poor as is evident from Fig. 40. The improved model including the effect of particle diffusion gives a better agreement (within 35%) with the experimental data and also approximately predicts q_∞ as proportional to N^2. The later effect may be shown as follows. From Eqs. (60), (62) and (36)

$$u = \frac{D_p^2(\rho_p-\rho)g}{18\mu} Z_0 + 0.0613\frac{\sqrt{\tau_w g_c}}{\sqrt{\rho}}\left(\frac{D}{\nu}\right)^{2/3} \ell n\frac{c_w}{c_b} \tag{87}$$

$$u = k_1 N^2 + k_2 N^{1.45}$$

where k_1 and k_2 are two constants.

c. Effect of Liquid and Particle Density. The simple centrifugal force model predicts that q_∞ is proportional to $(\rho_p-\rho)$. However our run no. 232 clearly contradicts that. We do not have enough data (with different ρ_p & ρ) to empirically establish the dependence of q_∞ on $(\rho_p-\rho)$. In the case when $(\rho_p-\rho)$ was negative (run no. 232) the diffusion term in Eq. (87) is positive and larger than the centrifugal term. The experimental result for this case is a persuasive argument in support of the diffusion effect.

Liquid density ρ and viscosity μ appear in the expression for q_∞ in the following form.

$$u = \frac{D_p^2(\rho_p-\rho)g}{18\mu} Z_0 + \frac{0.0613\sqrt{\tau_w g_c}\rho^{1/6}D^{2/3}}{\mu^{2/3}} \ln\frac{c_w}{c_b} \qquad (88)$$

From Eq. (88), q_∞ will decrease with increasing liquid viscosity.

2. Limitations of the Theory and the Predicted Results

From the previous discussion it is clear that the diffusion model gives a very satisfactory explanation of the phenomenon of limiting filtration rate as observed in this series of experiments. Agreement with experimental data within 35% seems quite satisfactory considering the assumptions and approximations made in developing this model. The diffusion term u_d in Eq. (62) is quite sensitive to the assumed expression for the growth of eddy diffusivity in the turbulent flow in rotating cylinders. We have here used the expression for eddy diffusivity developed by Wasan, Tien, and Wilke[20] for turbulent flow in circular pipes. If the correct expression for the eddy diffusivity ϵ were available for flow between two rotating cylinders, a better agreement between theory and experiments could be expected.

The diffusion model can be successfully used to design such a filter provided system properties including smallest particle size, particle density and liquid density, and viscosity are available.

ACKNOWLEDGMENTS

Thanks are due Professor Richard Ayen and Professor Wilbur Somerton for their invaluable aid and advice, and to Milton Moebus for fabricating the filter.

The work described was performed in the Lawrence Radiation Laboratory under the auspices of the U. S. Atomic Energy Commission.

APPENDIX A

Nomenclature and Units

a	constant in Eq. (29)
A	filter area (cm^2)
A	factor defined by Eq. (50) (cm)
A_p	projected area of the particle in the direction of motion (cm^2)
B	factor defined by Eq. (85) (sec/ml)
c_b	weight fraction of solids in the bulk of slurry
c_w	weight fraction of solids in the bulk of cake
c	weight fraction of solids
C_d	drag coefficient for particles
C_D	drag coefficient for rotating cylinders
d	gap width (cm)
D	molecular diffusivity of particles (cm^2/sec)
D_i	diam of the inner rotor (cm)
D_o	diam of the outer cylinder
F_c	centrifugal force (g_f)
F_d	drag force (g_f)
g	acceleration due to gravity (cm/sec^2)
G	torque (g_f cm)
h	height of the cylinder (cm)
k	constant in Eq. (4)
k	Boltzman constant (ergs/^oC)
k'	factor defined by Eq. (9)
K	a constant in Eq. (1)
K_p	factor defined by Eq. (84) (sec/ml^2)
L	cake thickness (cm)
m	an index in Eq. (5)
n	an index in Eq. (4)
n_p	mass flux of particles (g/sec cm^2)
n_ℓ	mass flux of liquid (g/sec cm^2)

P	pressure in outer cylinder (g_f/cm^2)
P_c	centrifugal pressure (g_f/cm^2)
P_o	discharge pressure (g_f/cm^2)
P_τ	power loss due to shear stress (watts)
ΔP	effective pressure drop across the membrane and cake (g_f/cm^2)
ΔP_{cl}	centrifugal pressure loss (g_f/cm^2)
ΔP_{ll}	pressure loss in liquid lines (g_f/cm^2)
q	rate of filtration/area (ml/sec cm^2)
q_o	initial filtration rate/area (ml/sec cm^2)
q_∞	limiting filtration rate/area (ml/sec cm^2)
Q	filtration rate (ml/sec)
Q_o	initial filtration rate (ml/sec)
Q_∞	limiting filtration rate (ml/sec)
R	total cake resistance (g_f sec/ml)
R_o	membrane resistance (g_f sec/ml)
R_m	membrane resistance as defined by Eq. (3) (cm^{-1})
r	radial distance (cm)
s_p	surface area of a single particle (cm^2)
T	temperature (^oK)
T	Taylor number as defined by Eq. (63)
u	superficial liquid velocity through the cake (cm/sec)
u_d	diffusion term in the limiting filtration rate/area as defined by Eq. (61)/(cm/sec)
u_t	terminal velocity of the particle under the centrifugal force (cm/sec)
u_{to}	terminal velocity of the particle at the membrane surface (cm/sec)
v	tangential velocity of liquid (cm/sec)
v'	tangential velocity of liquid relative to the membrane (cm/sec)
v_o	tangential velocity of the membrane (cm/sec)
v_p	volume of a single particle (cm^3)

V	volume of filtrate (ml)
w	dry weight of cake/area (g/cm^2)
W	dry weight of cake (g)
x	distance away from the membrane (cm)
x^+	dimensionless distance as defined by Eq. (26)
Z	centrifugal effect factor
Z_0	centrifugal effect factor at the membrane surface
Re_p	Reynold's number based on particle diam $(D_p u)/\nu$
Re_D	Reynold's number based on rotor diam $(v_o D_i)/(2\nu)$

Greek Letters

α	specific cake resistance (cm/g)
β	thickness coefficient of cake resistance (g_f sec/ml cm)
β'	cake resistance/(weight of dry cake/area)(g_f sec/g cm)
μ	viscosity of filtrate (poise)
ϵ	porosity of cake
ϵ'	eddy diffusivity (cm^2/sec)
ϵ_0	coefficient in Eq. (46)($sec^{-1}cm^{-1}$)
ρ	density of liquid (g/cm^3)
ρ_c	density of dry cake (g/cm^3)
ρ_s	density of slurry (g/cm^3)
ρ_p	density of particle (g/cm^3)
ω	angular velocity (radians/sec)
ω_0	angular velocity at the membrane surface (radians/sec)
τ	shear stress (g_f/cm^2)
ϕ	centrifugal pressure loss factor
ν	kinematic viscosity (cm^2/sec)
θ	time (sec)
δ	boundary layer thickness (cm)

APPENDIX B.

Sample calculations

Sample calculations of the limiting filtration rate/area, q_∞, for run number 120 for 1.3 micron slurry at 1000 rpm are shown below. system properties are:

$\rho_p = 1.056$ g/ml $\qquad \rho = 0.997$ g/ml

$D_p = 1.3$ micron $\qquad D_i = 6$ in.

$\mu = 0.894$ cp $\qquad N = 1000$

$c_b = 0.95 \times 10^{-3} \qquad c_w = 0.509$

$Z_0 = 84.8$

From Eq. (81)

$$\tau_w = 2.01 \times 10^{-9}(1000)^{2.9} = 0.988 \ g_f/cm^2$$

From Eq. (30)

$$a = \frac{0.988 \times 981 \times 60}{0.894 \times 10^{-2} \times \pi \times 6 \times 2.54 \times 1000}$$

$$= 136 \ cm^{-1}$$

From Eq. (54)

$$\delta = \frac{1}{2a} = 1/2 \times 136 \quad = 36.8 \times 10^{-4} \text{ cm}$$

From Eq. (47)

$$\epsilon_0 = \frac{4.16 \times 10^{-4}}{(0.894 \times 10^{-2})^2} \left(\frac{0.988 \times 981}{0.997} \right)^{3/2} = 1.57 \times 10^{-5} \ cm^{-1} sec^{-1}$$

From Eq. (48)

$$D = \frac{298 \times 1.37 \times 10^{-16}}{6 \times \pi \times 0.894 \times 10^{-2} \times 0.65 \times 10^{-4}} = 3.74 \times 10^{-8} \text{ cm}^2/\text{sec}$$

From Eq. (50)

$$A = \left(\frac{D}{\epsilon_0}\right)^{1/3} = \left(\frac{3.74 \times 10^{-8}}{1.57 \times 10^{5}}\right)^{1/3} = 0.628 \times 10^{-4} \text{ cm}$$

From Eq. (36)

$$u_{t0} = \frac{(1.34 \times 10^{-4})^2 \ (1.056 - 0.997) \ 980 \times 84.8}{18 \times 0.894 \times 10^{-2}}$$

$$= 4.78 \times 10^{-4} \text{ cm/sec}$$

From Eq. (61)

$$u_d = \frac{3\sqrt{3}}{2\pi} A^2 \epsilon_0 \ln \frac{c_w}{c_b}$$

$$= \frac{3\sqrt{3}}{2\pi} (0.628 \times 10^{-4})^2 \ 1.57 \times 10^{5} \ln \frac{0.509}{0.95 \times 10^{-3}}$$

$$= 3.2 \times 10^{-3} \text{ cm/sec}$$

Therefore

$$u = q_\infty = 4.78 \times 10^{-4} + 3.2 \times 10^{-3}$$

$$= 3.68 \times 10^{-3} \text{ cm/sec}$$

References

1. Bachelor, G. K., J. Fluid Mech. 1, 177 (1956).
2. Bird, R B., Stewart, W. E., and Lightfoot, E. N., Transport Phenomena, (john Wiley and Sons Inc., New York, 1960), p. 502.
3. Carman, Trans. Inst. Chem. Eng. (london), 16, 174 (1938).
4. Chandrasekhar, S., Proc. Roy, Soc. A246, 301 (1958).
5. Daniels, W. F. and Malcom B. Hale, J. Biochem. Microbiol. Tech. Eng., II, No. 1, 93 (1960).
6. Donnely, R. J., J. Fluid Mech. 7, 401 (1960).
7. Dwight, H. B., Tables of Integrals and Other Mathematical Data, (Macmillan, New York, 1961).
8. The Eaton-Dikeman Company, Hand Book of Filtration (Filter Town, Pennsylvania, 1960) p. 3.
9. Eisenberg, M., Tobias, C. W., and C. R. Wilke, Chem. Eng. Prog. Sym. Series No. 16, Vol. 51.
10. Grace, H. P., A. I. Ch. E. J. 2, 307 (1956).
11. Hermans, P. H. and Bredee, H. L., Rec. Trav. Chim. 54, 680 (1935).
12. Hermans, P. H. and Bredee, H. L., J. Soc. Chem. Ind. London 55, 1T (1936).
13. McCabe and Smith, Unit Operations of Chemical Engineering (McGraw-Hill Book Co., Inc., New York, 1956).
14. Perry, John H., Chemical Engineers Hand Book, 4th Ed., (McGraw-Hill Book Co., Inc., New York, 1963), p. 5.
15. Perry, John H., Chemical Engineers Hand Book, 4th Ed., (McGraw-Hill Book Co., Inc., New York, 1963), 19.
16. Schlicting, H., Boundary Layer Theory, (McGraw,Hill Book Co., Inc., New York,), 355 and 359.
17. Taylor, G. I., Proc. Roy. Soc. A157, 546 (1936).
18. Theodorsen, T. and Regeir, A., Natl. Advisory Comm. Aeronaut. Rpt., 793 (1944).

19. Von Karman, T., Trans. Am. Soc. Mech. Eng. 61, 705 (1939).

20. Wasan, D. T., Tien, C. L., and Wilke, C. R., A. I. Ch. E. J. 9, 567 (1963).

21. Wilke, C. R. and P. Chang, A. I. Ch. E. J. 1(2), 270 (1955).